

From the First Selective Non-Peptide AT₂ Receptor Agonist to Structurally Related Antagonists

A. M. S. Murugaiah,[†] Xiongyu Wu,[†] Charlotta Wallinder,[†] A. K. Mahalingam,[†] Yiqian Wan,[†] Christian Sköld,[†] Milad Botros,[§] Marie-Odile Guimond,[‡] Advait Joshi,[†] Fred Nyberg,[§] Nicole Gallo-Payet,^{*,‡} Anders Hallberg,^{*,†} and Mathias Alterman^{*,†}

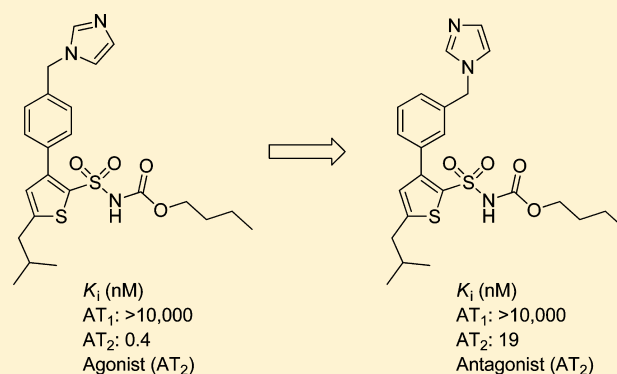
[†]Department of Medicinal Chemistry, BMC, Uppsala University, P.O. Box 574, SE-751 23 Uppsala, Sweden

[‡]Service of Endocrinology and Department of Physiology and Biophysics, Faculty of Medicine, University of Sherbrooke, Sherbrooke J1H 5N4, Quebec, Canada

[§]Department of Biological Research on Drug Dependence, BMC, Uppsala University, P.O. Box 591, SE-751 23 Uppsala, Sweden

S Supporting Information

ABSTRACT: A para substitution pattern of the phenyl ring is a characteristic feature of the first reported selective AT₂ receptor agonist M024/C21 (**1**) and all the nonpeptidic AT₂ receptor agonists described so far. Two series of compounds structurally related to **1** but with a meta substitution pattern have now been synthesized and biologically evaluated for their affinity to the AT₁ and AT₂ receptors. A high AT₂/AT₁ receptor selectivity was obtained with all 41 compounds synthesized, and the majority exhibited K_i ranging from 2 to 100 nM. Five compounds were evaluated for their functional activity at the AT₂ receptor, applying a neurite outgrowth assay in NG108-15 cells. Notably, four of the five compounds, with representatives from both series, acted as potent AT₂ receptor antagonists. These compounds were found to be considerably more effective than PD 123,319, the standard AT₂ receptor antagonist used in most laboratories. No AT₂ receptor antagonists were previously reported among the derivatives with a para substitution pattern. Hence, by a minor modification of the agonist **1** it could be transformed into the antagonist, compound **38**. These compounds should serve as valuable tools in the assessment of the role of the AT₂ receptor in more complex physiological models.



INTRODUCTION

The octapeptide angiotensin II (Ang II) is the main effector of the renin–angiotensin system (RAS) and exerts its effects via activation of two receptors, AT₁ and AT₂. Activation of the AT₁ receptor is associated with the well-known functions of the RAS such as regulation of blood pressure and fluid/electrolyte balance. In contrast, the physiological role of the AT₂ receptor and the impact of its stimulation are less well understood.^{1,2} This may be due to the low expression of the AT₂ receptor in healthy adults where it is localized to specific tissues such as the heart, ovary, kidney, and some areas of the brain.^{1,3} Prior to birth, the AT₂ receptor is the predominant Ang II receptor, suggesting that it plays a role in fetal development.^{4,5} Notably, the AT₂ receptor is up-regulated in adults during certain pathological conditions such as vascular, skin, and axonal injury, renal damage, myocardial infarction, and brain ischemia.^{6–11} It is postulated to be involved in wound healing and tissue repair and to act anti-inflammatory.^{7,11–15} The AT₂ receptor mediates cell differentiation, apoptosis, and alkaline secretion in the duodenal mucosa¹⁶ and frequently exerts opposing effects to the AT₁ receptor; for example, it promotes antiproliferation and

vasodilatation.^{1,3,17–20} Recently, the AT₂ receptor has emerged as a potential target for pharmaceutical agents. In 2004, we disclosed the first druglike selective AT₂ receptor agonist M024/C21 (**1**),⁵⁶ which displayed reasonable bioavailability after oral administration (Figure 1).²¹ It demonstrated remarkable beneficial effects on heart function after myocardial infarction in rats, and its potential use for the treatment of heart failure was recently discussed and reviewed.^{22–24} Compound **1** is the most selective AT₂ receptor agonist reported to date and represents a unique tool to delineate the specific roles of the AT₂ receptor in different cellular and animal models.^{25,26} Furthermore, stimulation of the AT₂ receptor with intracerebroventricular administered N_α-nicotinoyl-Tyr-(N_α-Cbz-Arg)-Lys-His-Pro-Ile (CGP-42112A), a selective but peptidic AT₂ receptor agonist,^{27,28} is known to exhibit a neuroprotective effect in a model of stroke in conscious rats.¹³

We have synthesized a series of compounds related to **1** but with a meta rather than a para substitution pattern at the phenyl

Received: November 8, 2011

Published: January 16, 2012

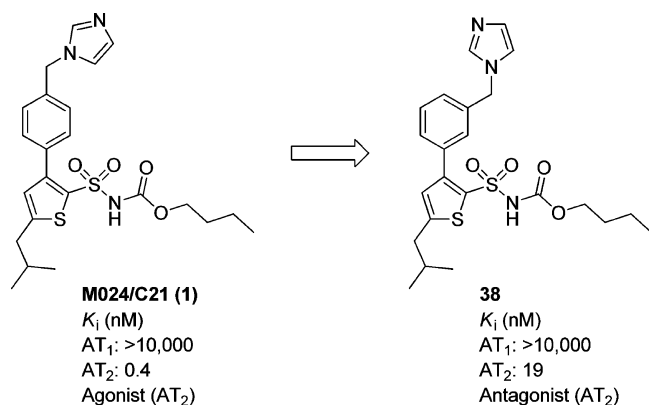


Figure 1.

ring. Herein we report that by this migration of substituents, as exemplified by the transformation of **1** to **38**, the AT_2 receptor agonism could be converted into AT_2 receptor antagonism (Figure 1).

DESIGN

The first druglike selective AT_2 receptor agonist **1** was derived from the nonselective AT_1/AT_2 receptor ligand L-162,313 (**2**) (Figure 2).²¹ Ligand **2** was identified as an AT_1 receptor agonist 2 decades ago^{29,30} and was thereafter shown by us to also act as an agonist at the AT_2 receptor.³¹ Compound **2** is a thiophene analogue of the nonselective AT_1 receptor agonist L-162,782 (**3**), which is structurally very similar to the nonselective AT_1

receptor antagonist L-162,389 (**4**) (Figure 2).³² Notably, the only difference between **3** and **4** is the methyl group in the alkyl chain.

By systematic modification of the N-heterocyclic moiety of **2**, improved AT_2 receptor selectivity was achieved and the imidazole derivative **1** was eventually obtained.²¹ Considerable efforts have been devoted to identifying selective AT_2 receptor agonists,^{33–38} and several series of analogues of **1** were synthesized and biologically evaluated.^{39–42} Among those analogues, compound **5** was found to act as an AT_2 receptor agonist despite the fact that the molecule is lacking a methyl group in the alkyl chain (cf. the AT_1 receptor agonist **3** vs the AT_1 receptor antagonist **4**, Figure 2).³⁹ The main structural features of the compound class originating from **1** are the imidazole ring, the sulfonyl carbamate substituent, and the isobutyl chain all attached to a bicyclic scaffold. Structural modifications of both the sulfonyl carbamate substituent and the isobutyl group had in general a negative impact on the binding affinity. In contrast, diverse substituents in the benzylic position were often accepted and both substituted nitrogen-containing aromatic heterocycles and linear amides were proven to produce selective AT_2 receptor ligands with high affinities and potent agonistic effects. Furthermore, substituting the phenyl ring for a furan ring rendered the receptor selective compound **6** (Figure 2) with similar affinity and retained functional activity, though the substitution pattern in the furan ring more resembles a “meta” rather than a “para” configuration.⁴⁰ Hence, these findings encouraged us to assess the effects of switching the substituted methylene group from

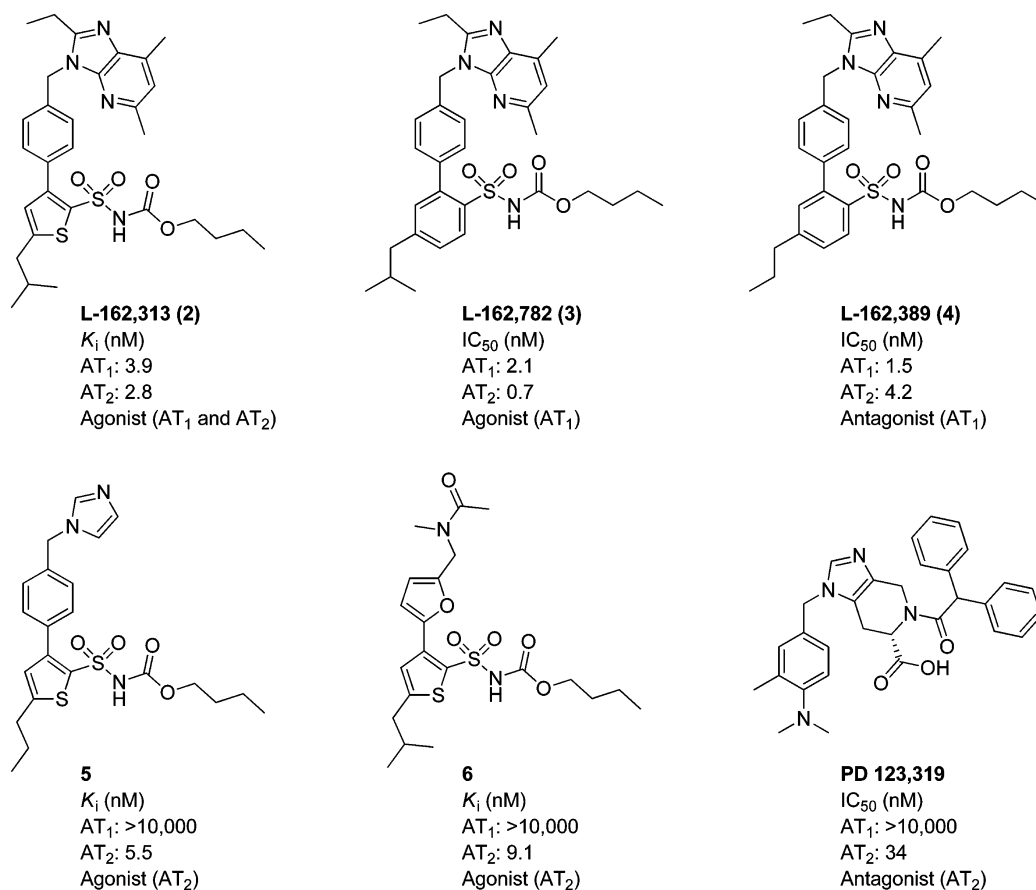
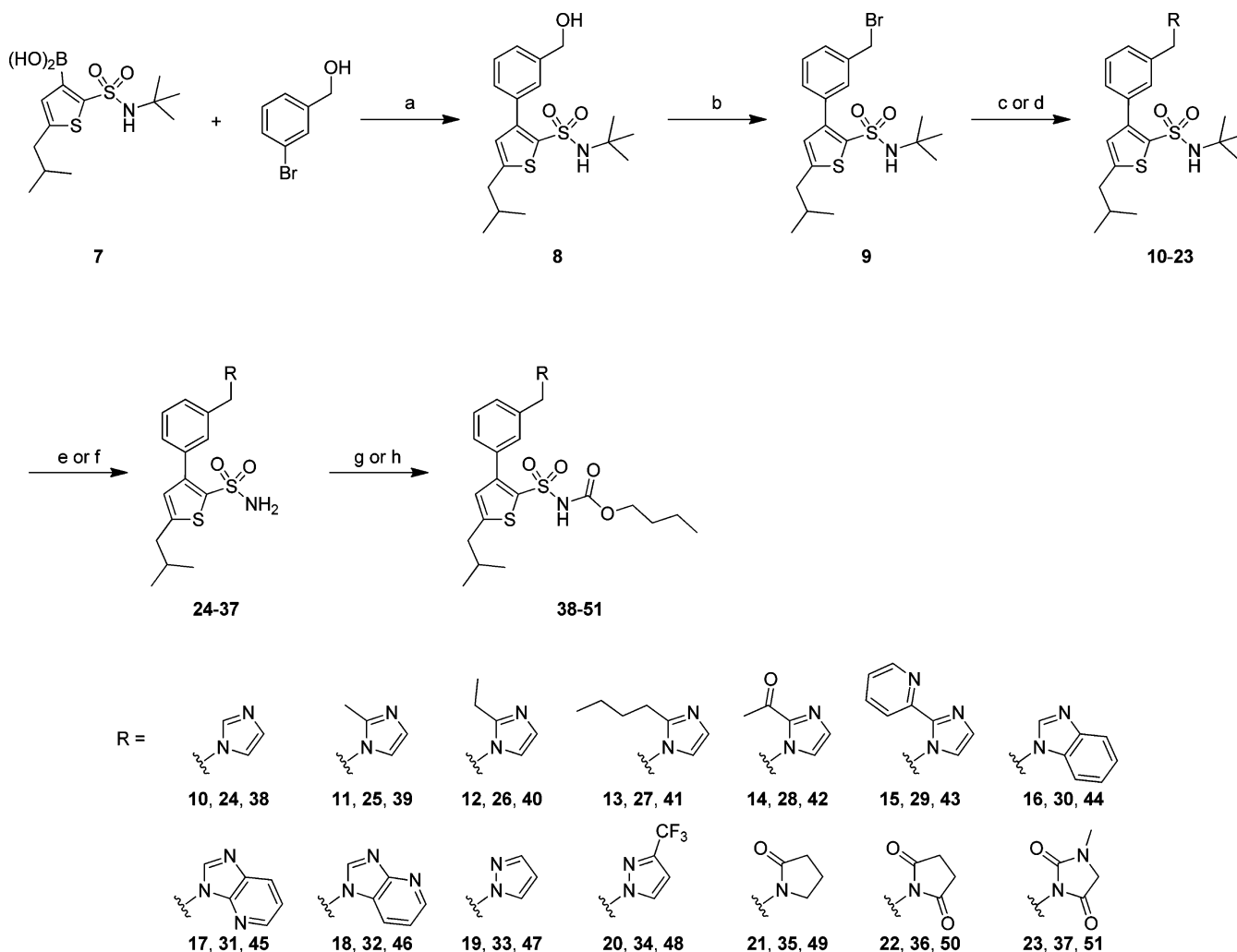
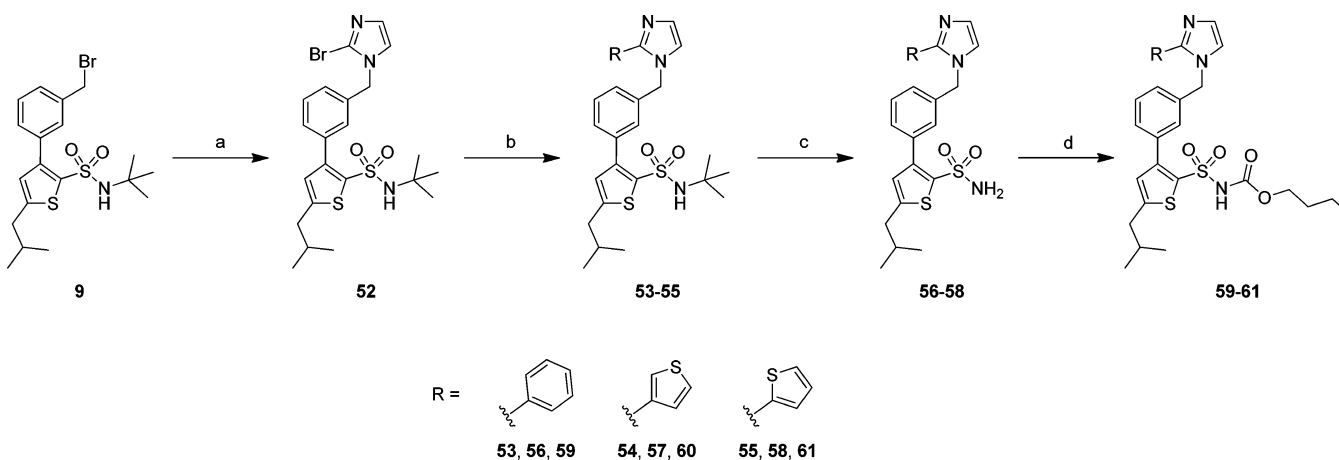


Figure 2.

Scheme 1^a

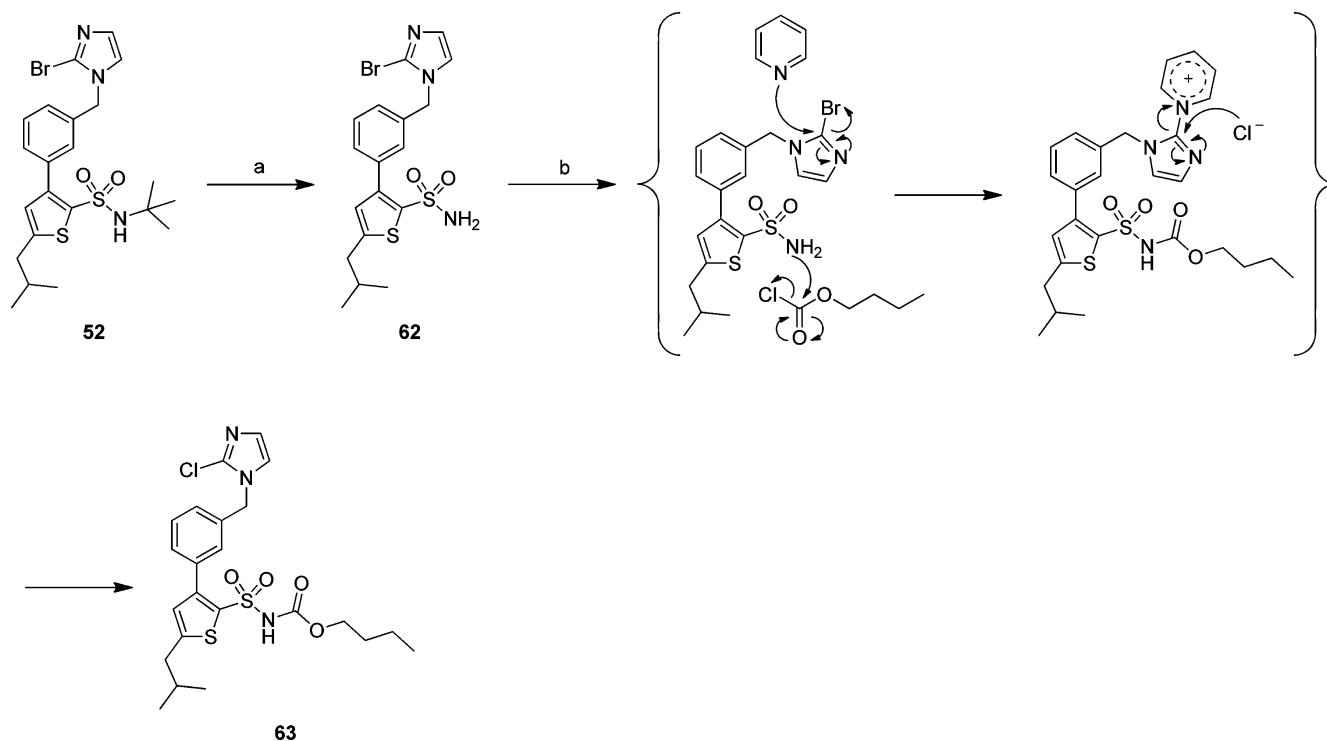
^aReagents: (a) Pd(PPh₃)₄, NaOH, toluene, EtOH; (b) CBr₄, PPh₃, DMF; (c) heterocycle, 1,4-dioxane (10–13, 16, 19); (d) heterocycle, DMSO, base (14, 15, 17, 18, 20–23); (e) BCl₃, DCM (24–27, 29–37); (f) TFA, anisole (28); (g) *n*-butyl chloroformate, pyrrolidinopyridine, pyridine (38, 40, 44–51); (h) *n*-butyl chloroformate, Na₂CO₃, DCM, H₂O (39, 41–43).

Scheme 2^a

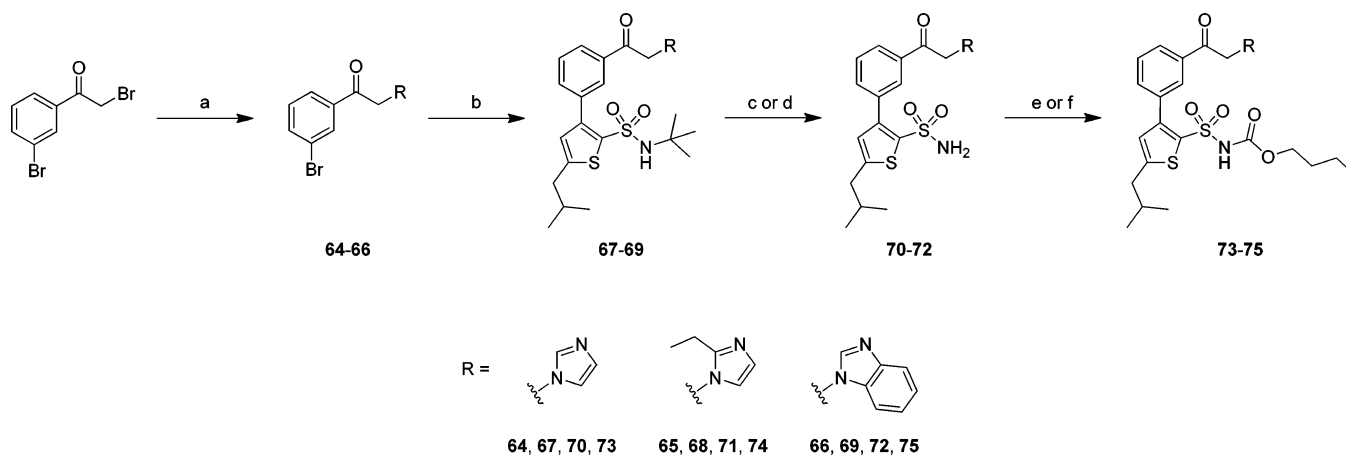
^aReagents: (a) 2-bromoimidazole, DMSO, NaOH; (b) boronic acid, Pd(PPh₃)₄, NaOH, toluene, EtOH (53, phenylboronic acid; 54, 3-thiophenylboronic acid; and 55, 2-thiophenylboronic acid); (c) BCl₃, DCM; (d) *n*-butyl chloroformate, Na₂CO₃, DCM, H₂O.

the para position to the meta position of the phenyl ring. We were intrigued to see whether these analogues would retain

high affinity and, if so, how the functional activity at the AT₂ receptor would be affected. To address this question, two series

Scheme 3^a

^aReagents: (a) TFA, anisole; (g) *n*-butyl chloroformate, pyrrolidinopyridine, pyridine.

Scheme 4^a

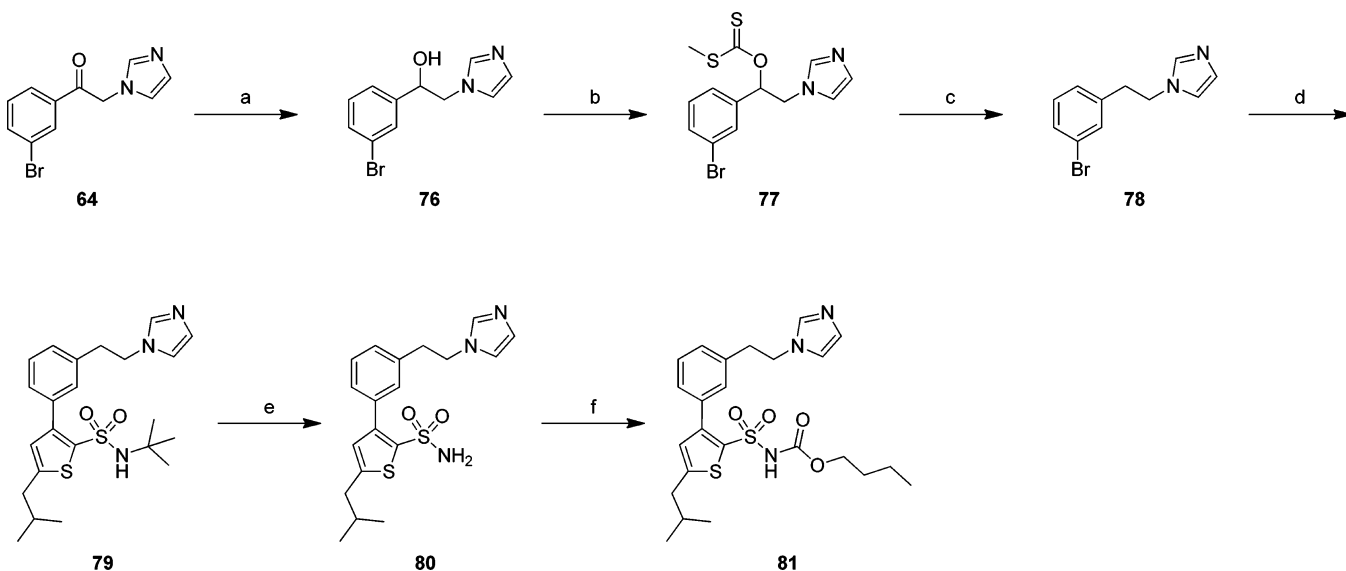
^aReagents: (a) heterocycle, dioxane (64, imidazole; 65, 2-ethylimidazole; and 66, benzimidazole); (b) boronic acid 7, Pd(PPh₃)₄, Na₂CO₃, toluene, EtOH; (c) BCl₃, DCM (70); (d) TFA, anisole (71, 72); (e) *n*-butyl chloroformate, Na₂CO₃, DCM, H₂O (73, 74); (f) *n*-butyl chloroformate, pyrrolidinopyridine, pyridine (75).

of compounds were synthesized and biologically evaluated. PD 123,319, used as a standard AT₂ receptor antagonist with an IC₅₀ of 34 nM, is depicted for structural comparison in Figure 2.^{27,43}

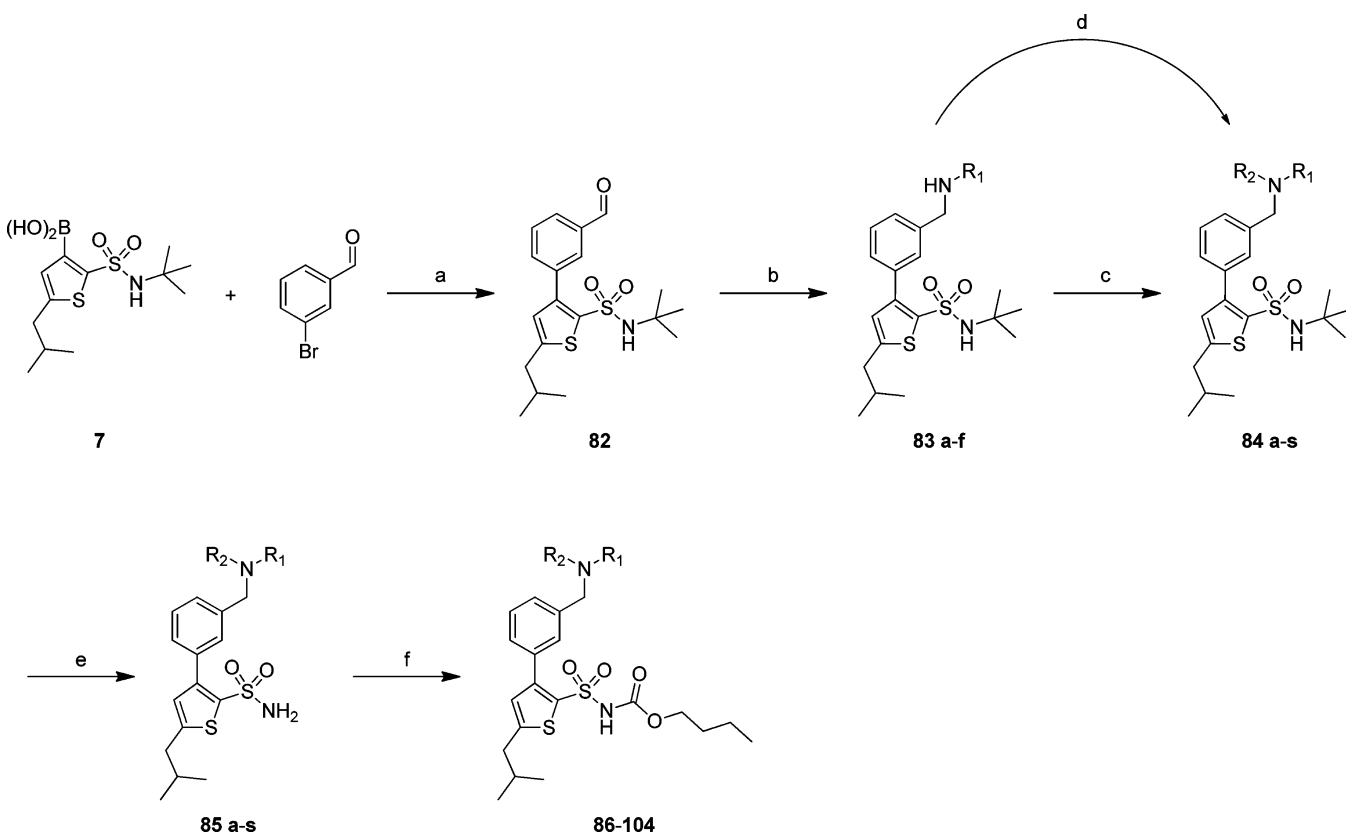
RESULTS

Chemistry. The synthesis of all compounds commenced with the thiopheneboronic acid 7, which was prepared in essence as previously described by Kevin et al.⁴⁴ The synthesis of compounds 38–51, series 1 (Scheme 1), were executed via a Suzuki coupling of thiopheneboronic acid 7 and 3-bromobenzyl alcohol with palladium tetrakis as catalyst and NaOH as base to

obtain the benzyl alcohol 8 in a modest yield. The benzyl alcohol was successfully converted to the corresponding bromide 9 in a high yield, a key intermediate in the synthesis of series 1. The bromide 9 was reacted with the selected heterocycles to give the desired compounds 10–23 in moderate to high yields (51–99%). Compounds 17 and 18 were obtained simultaneously upon reacting 9 with imidazopyridine, and the two regioisomers were separated to afford the desired compounds in 19% and 49% yield, respectively. The final compounds 38–51 were obtained after deprotection of the *tert*-butyl group⁴⁵ and subsequent coupling of the free sulfonamide with *n*-butyl chloroformate in modest to good yield (Scheme 1).

Scheme 5^a

^aReagents: (a) (i) NaBH₄, MeOH, (ii) H₂O, DCM, HCl_(aq); (b) NaH, THF, CS₂, MeI; (c) Bu₃SnH, THF, AIBN; (d) boronic acid 7, Pd(PPh₃)₄, Na₂CO₃, toluene, EtOH; (e) BCl₃, DCM; (f) *n*-butyl chloroformate, Na₂CO₃, DCM, H₂O.

Scheme 6^a

^aReagents: (a) Pd(OAc)₂, PPh₃, K₂CO₃, THF/DME/EtOH/H₂O; (b) amine, NaBH₄, MeOH; (c) acid chloride, NEt₃, DMAP, DCM; (d) ammonium formate, MeCN; (e) TFA, anisole; (f) *n*-butyl chloroformate, NEt₃, pyrrolidinopyridine, DCM. R₁ and R₂: See Table 2 for details.

Compounds 59–61 in series 1 were derived from the alkylation of 2-bromimidazole with compound 9 to obtain the intermediate 52 in excellent yield (Scheme 2). The *N*-alkylated 2-bromimidazole 52 was then coupled with three different arylboronic acids in Suzuki reactions with palladium tetrakis as catalyst and NaOH as base to form intermediates 53, 54, and

55, respectively, in modest to good yields. Subsequent deprotection and reaction with *n*-butyl chloroformate rendered the final compounds 59–61 in 55–87% yield.

The chloroimidazole derivative (63) was obtained from compound 52. Most likely the bromide was substituted by pyridine which subsequently was substituted by a chloride,

Table 1. Binding Affinity of Series 1 to the AT₂ Receptor

Entry	Compound	R	K _i (nM) ^{a, b}	Entry	Compound	R	K _i (nM) ^{a, b}
1	38		19	12	45		66
2	63		9.2	13	46		44
3	39		29	14	47		110
4	40		8.0	15	48		233
5	41		10	16	49		224
6	42		17	17	50		147
7	59		67	18	51		37
8	43		28	19	73		22
9	61		28	20	74		12
10	60		33	21	75		20
11	44		32	22	81		118

^aK_i values are an average from three determinations. Standard deviations are less than 15% in all cases. ^bAll compounds were evaluated for binding toward the AT₁ receptor, and all compounds exhibited K_i > 10 000 nM.

generated when the intermediate **62** was treated with pyridine and *n*-butyl chloroformate (Scheme 3).

Compounds **73–75** (Scheme 4), with a carbonyl-extended chain between the phenyl and the imidazole, were synthesized by *N*-alkylation of the appropriate heterocycle with 2-bromophenacyl bromide giving compounds **64–66** in moderate yields. The formed bromides were coupled with the thiopheneboronic acid **7** under Suzuki conditions with

palladium tetrakis as catalyst and sodium carbonate as base in excellent yields. Compounds **67–69** were treated with TFA or BCl₃ to deprotect the sulfonamide and subsequently with *n*-butyl chloroformate to obtain the final compounds **73–75**.

The final compound in the first series, **81** (Scheme 5), was achieved by reduction of the carbonyl group of **64**. Initially the carbonyl was reduced to the corresponding alcohol with sodium borohydride. Reaction of the alcohol **76** with sodium

hydride, carbon disulfide, and methyl iodide formed the *S*-methyl carbonodithioate **77** in excellent yield (99%). Treatment of compound **77** with Bu_3SnH and AIBN rendered compound **78** in modest yield. The boronic acid **7** was coupled with **78** in a Suzuki reaction with palladium tetrakis as palladium source and Na_2CO_3 as base to yield compound **79**. Deprotection of **79** with BCl_3 and subsequent reaction with *n*-butyl chloroformate gave the final compound **81** in good yield.

The synthesis of series 2, as outlined in Scheme 6, originated with the coupling of thiopheneboronic acid **7** with 3-bromobenzaldehyde in a Suzuki reaction with palladium acetate as precatalyst, PPh_3 as ligand, and K_2CO_3 as base to obtain the aldehyde **82**. The final compounds **86–104** were then prepared in a combinatorial fashion where the key intermediate (**82**) was dissolved in methanol and added to sample vials. A diverse set of amines were dispensed to the vials, and after the samples were stirred for 30 min, NaBH_4 was added to achieve the reductive amination with full conversion. The workup was performed by solid–liquid extraction through a diatomaceous earth plug in a polypropylene column with ethyl acetate as eluent. The secondary amines (**83a–f**) were used in the third step without further purification. The crude products **83a–f** were dissolved in dichloromethane, and triethylamine and DMAP were added. Acid chlorides were added to the reaction vials, and the mixtures were stirred for 2 h. The same solid–liquid extraction workup, as in the previous step, was used again to obtain the crude amides (**84b–s**) in high yields and high purity. The formyl compound **84a** was synthesized by refluxing the secondary amine **83a** with ammonium formate. In the final steps the *tert*-butyl protecting group was removed from the sulfonamide with TFA and the free sulfonamide was subsequently reacted with *n*-butyl chloroformate to yield the final products **86–104** in 41–86% overall yield after purification on preparative HPLC.

Binding Assays. The final products were evaluated in radioligand assays by displacement of [^{125}I]Ang II from AT_1 receptors in rat liver membranes and from AT_2 receptors in pig uterus membrane as previously described.^{46,47} The selective AT_1 receptor antagonist losartan and the natural ligand Ang II were used as reference substances. The results are summarized in Tables 1 and 2.

In series 1, containing substituted heterocycles (Table 1), all compounds showed affinity to the AT_2 receptor and did not bind to the AT_1 receptor ($K_i > 10\,000$ nM). Compound **38**, the meta substituted analogue of **1**, exhibited an affinity of 19 nM to the AT_2 receptor. Introducing a 2-chloro substituent on the imidazole ring resulted in higher affinity (**63**, $K_i = 9.2$ nM). Alkyl substituents in the 2-position of the imidazole ring gave compounds with similar affinities, whereas a methyl group rendered decreased affinity (**39**, $K_i = 29$ nM) but prolongation of the chain to an ethyl or *n*-butyl resulted in increased affinities (**40**, $K_i = 8.0$ nM or **41**, $K_i = 10$ nM, respectively). An acetyl substituent in this position was accepted with no significant effect on binding affinity compared to **38**. Introducing aromatic/heteroaromatic rings as substituents in the 2-position of the imidazole ring gave compounds with lower affinity (**43**, **59–61**), but the decrease in affinity was not as profound with heteroaromatic substituents compared to what was encountered with a phenyl substituent. Replacing the imidazole with bicyclic heteroaromatic rings gave compounds (**44–46**) that showed reduced affinity for the AT_2 receptor. Notably, replacing imidazole with pyrazole, that is, moving the nitrogen atom one position in the ring, diminished the affinity 5-fold (**38**

Table 2. Binding Affinity of Series 2 to the AT_2 Receptor

Entry	Compound	R ₁	R ₂	K_i (nM) ^{a,b}
1	86			55
2	87			29
3	88			56
4	89			45
5	90			1.6
6	91			13
7	92			> 10,000
8	93			29
9	94			72
10	95			120
11	96			79
12	97			83
13	98			46
14	99			35
15	100			47
16	101			670
17	102			2.2
18	103			133
19	104			163

^a K_i values are an average from three determinations. Standard deviations are less than 15% in all cases. ^bAll compounds were evaluated for binding toward the AT_1 receptor, and all compounds exhibited $K_i > 10\,000$ nM.

vs **47**). Introducing a trifluoromethyl group in the 3-position of the pyrazole resulted in further decline in affinity (**48**).

Insertion of a carbonyl group to extend the distance between the phenyl ring and the imidazole ring had no effect on binding affinity (cf. **73** vs **38**, **74** vs **40**, and **75** vs **44**), and reduction of the carbonyl in compound **73**, rendered the etylenimidazole **81** with lower affinity. Finally, the aromatic heterocycles were replaced with saturated nitrogen-containing heterocycles as in **49–51**. Compounds **49** and **50** exhibited low affinity to the AT₂ receptor, but the hydantoin **51** showed that some affinity could be regained.

In the second series of compounds, tertiary amide-based substituents in the 3-position of the phenyl ring were investigated (Table 2). As in the first series none of the compounds showed AT₁ receptor affinity. The formamide based compound **86** exhibited affinity to the AT₂ receptor with a K_i of 55 nM. Extending the R₂ chain, exemplified by the amide and carbamate substituents of compounds **87–89**, did not substantially affect the binding affinities. However, insertion of a carbonyl group in **89** to afford **90** (K_i = 1.6 nM) resulted in a significantly improved binding affinity, and introduction of a thiophene in the amide substituent was also well-tolerated by the AT₂ receptor (**91**, K_i = 13 nM). Notably, the sulfonamide substituent in **92** completely abolished the binding affinity, which was surprising considering the relatively small structural difference compared to **87**.

Varying R₁ did not improve the AT₂ receptor affinity in the compounds with acetamide-based substituents (**87** and **93–97**). Altering the alkyl group, that is, a methyl to an ethyl, had no impact on binding affinity (cf. **87** vs **93**), and replacing the terminal hydrogen atoms for fluorine (**93** vs **94**) decreased the affinity, which also was the case when the size of R₁ was made larger by introducing aromatic rings (**95–97**). A 2-fold improvement in affinity was observed with compounds with aromatic groups in R₁ and larger size groups in R₂ (**98–100** vs **95–97**). Notably, the introduction of a thiophene ring in R₂ and benzyl as R₁ did lower the affinity (**101** vs **96**) while a better affinity was observed with ethyl as R₁ (**102** vs **101**). The sulfonamide unit in **92** rendered the compound inactive, but by extension of R₂ with a thiophene ring and by increase of the size of R₁ to an ethyl, some of the affinity was recovered (**103**, K_i = 133 nM). Attachment of a cyclopropyl ring to R₂ in compound **94** also reduced the affinity (**104**).

In Vitro Morphological Effects of 38, 63, 75, 90, and 100 in NG108-15 Cells. A set of five high-affinity and structurally diverse compounds (**38**, **63**, **75**, **90**, and **100**) were selected for evaluation of their functional activity at the AT₂ receptor, applying a neurite outgrowth assay in NG108-15 cells. We have previously shown that NG108-15 cells in their undifferentiated state express only the AT₂ receptor and that a 3-day treatment with Ang II or the selective peptidic AT₂ receptor agonist CGP-42112A induces neurite outgrowth.^{28,48} The signaling pathways involve a sustained increase in Rap1/B-Raf/p42/p44^{mapk} activity and activation of the nitric oxide/guanylyl cyclase/cGMP pathway.^{49–51} Cells were plated as described in the Experimental Section, and adequate test concentrations for each compound were determined by testing a dilution series of each compound ranging from 1 pM to 1 μM. For all the compounds it was only at the highest concentration that any evidence of cell death was observed. Cells were then treated in the absence or presence of Ang II (100 nM), **38** (10 nM), **63** (10 nM), **75** (10 nM), **90** (1 nM), and **100** (10 nM). After 3 days of treatment, cells were examined under a phase-contrast microscope and micrographs were taken. Antagonistic effect was verified through co-incubation with Ang II resulting

in reduced Ang II-induced neurite outgrowth, verifying blockage of the AT₂ receptor. Agonistic effect was verified through co-incubation with the selective AT₂ receptor antagonist PD 123,319 (Figure 2), which reduced neurite outgrowth, verifying that the effect was mediated through the AT₂ receptor. Treatment with PD 123,319 alone did not alter the morphology compared to untreated cells. The neurite outgrowth results are shown in Figures 3 and 4.

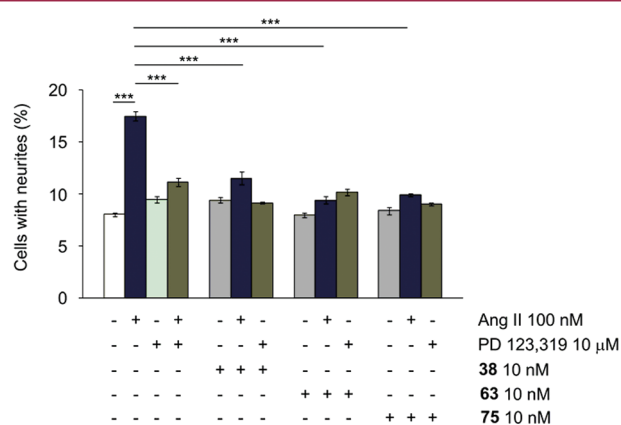


Figure 3. Effect of compounds **38**, **63**, and **75** on neurite outgrowth in NG108-15 cells. The cells were plated at a cell density of 3.6×10^4 cells/Petri dish (35 mm) and were cultured for 3 days in the absence (–) or presence (+) of 100 nM Ang II, 10 nM **38**, 10 nM **63**, or 10 nM **75** alone or in combination with 10 μM antagonist PD 123,319 or 100 nM Ang II. Cells with at least one neurite longer than a cell body were counted as positive for neurite outgrowth. The number of cells with neurites was expressed as the percentage of the total number in the micrographs (at least 290 cells according to the experiment). The results are significant according to two-way ANOVA: ***, $p < 0.001$.

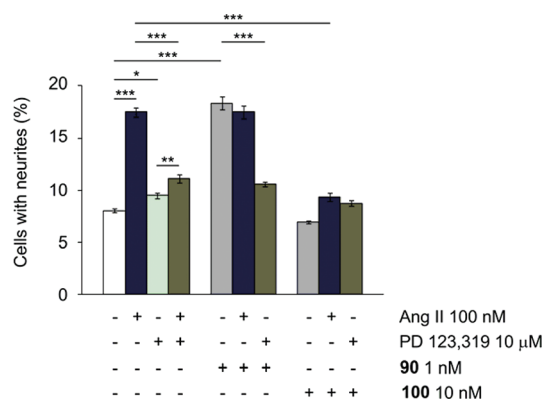


Figure 4. Effect of compounds **90** and **100** on neurite outgrowth in NG108-15 cells. The cells were plated at a cell density of 3.6×10^4 cells/Petri dish (35 mm) and were cultured for 3 days in the absence (–) or presence (+) of 100 nM Ang II, 1 nM **90**, or 10 nM **100** alone or in combination with 10 μM antagonist PD 123,319 or 100 nM Ang II. Cells with at least one neurite longer than a cell body were counted as positive for neurite outgrowth. The number of cells with neurites was expressed as the percentage of the total number in the micrographs (at least 290 cells according to the experiment). The results are significant according to two-way ANOVA: ***, $p < 0.001$; **, $p < 0.01$; *, $p < 0.05$.

The meta-analogue of **1**, compound **38** (10 nM), did not stimulate neurite outgrowth upon cell treatment, and pretreatment with 10 nM **38** reduced Ang II-induced neurite outgrowth from 17.5% to 11.5%, (Figure 3). These results

indicate that **38** exhibits antagonistic properties at the AT₂ receptor in contrast to the agonism exerted by **1**. Two more analogues from series 1 (**63** and **75**) were evaluated for functional activity, and none of the compounds induced neurite outgrowth, while pretreatment of the cells with either compound reduced Ang II-induced neurite outgrowth. Again, the antagonistic effect was achieved at the low concentration of 10 nM for both compounds (Figure 3). From series 2 compounds **90** and **100** were selected for determination of functional activity, and interestingly **90** (1 nM) showed agonistic activity while **100** (10 nM) followed the pattern from series 1 and exhibited antagonism (see Figure 4). All results were significant according to two-way analysis of variance (ANOVA).

DISCUSSION

The only nonpeptidic AT₂ receptor antagonist available is PD 123,319 (Figure 2), which serves as the standard substance in most studies on the AT₂ receptor.²⁶ Despite the good binding of PD 123,319 to the AT₂ receptor (an IC₅₀ of 34 nM), 10 μM was required to obtain a satisfactory inhibition of the Ang II stimulated neurite outgrowth in NG108-15 cells (1 μM PD 123,319 can be used to get inhibition of neurite outgrowth but with a high variability in the results), suggesting that the efficacy is far from optimal. Hence, due to the lack of other potent and effective AT₂ selective antagonists, there is a need for new more effective and robust antagonists.

There are several examples of subtle structural modifications in non-peptide ligands to peptide activated receptors that result in reversed functional response.^{52,53} In the case of the nonpeptidic ligands binding to the AT₁ receptor, the functional activity switches from antagonism to agonism when the isobutyl chain is exchanged to a *n*-propyl chain (**3** vs **4**; see Figure 2).³² The same transformation of the selective non-peptide AT₂ receptor agonist **1** does not alter the functional activity; the *n*-propyl analogue of **1** retains its agonistic properties (**5** in Figure 2).³⁹ In the present study it has been demonstrated that the functional switch of the AT₂ receptor ligands is related to the substitution pattern of the phenyl group rather than small variations in the lipophilic side chain. Thus, a transfer of substituent from the para-position (**1**) to the meta-position (**38**) interconverts the functional activity from agonism to antagonism. The meta substitution pattern thus seems to render ligands that retain affinity to the AT₂ receptor but lack the capacity to adopt conformations that allow interactions with the receptor that are required for its activation. Compared to the commercially available nonpeptidic AT₂ antagonist, PD 123,319, these new antagonists exerted good inhibition of Ang II-induced neurite outgrowth at a 1000-fold lower concentration. While the antagonist PD 123,319 was used at 10 μM to obtain a satisfactory inhibition of neurite outgrowth, the new antagonists exhibited good inhibition at 10 nM, that is, compounds **38**, **63**, **75**, and **100**. Even if these results are somewhat surprising at first glance, because of the low concentration, they were repeatedly observed and in this study, only neurite outgrowth was assessed, which is the final effect of AT₂ receptor in these cells. However, it is known that a partial inhibition of the signaling pathway is sufficient to completely impede neurite outgrowth. It has been observed, for example, that the TrkA inhibitor α -cyano-(3,5-di-*tert*-butyl-4-hydroxy)thiocinnamide (AG879)⁵⁴ only partially inhibits the p42/p44^{mapk} pathway but that its effect on neurite outgrowth is total.⁵⁵ In a similar manner, a partial occupation of AT₂

receptor binding sites by these new antagonists could induce partial inhibition of the signaling pathway and therefore inhibit Ang II-induced neurite outgrowth. Nevertheless, since the functional experiments were performed on intact cells, the possibility of interactions with other growth stimulating systems cannot be excluded.

Of the five compounds evaluated for functional activity at the AT₂ receptor, four (**38**, **63**, **75**, and **100**) acted as antagonists and inhibited Ang II-induced neurite outgrowth while one of them, compound **90**, functioned as a potent agonist. Compound **90** differs structurally from the four antagonists by having the longer and flexible α -keto ester substituent, compared to more bulky substituents in the antagonists (**38**, **63**, **75**, and **100**). A possible explanation of why compound **90** acts as an agonist despite the 1,3-substitution pattern is that either the flexibility or the oxoacetate function of the substituent can compensate for the substitution pattern. Thereby it can facilitate the interactions with the receptor required for activation that the more bulky substituents cannot achieve. It is less likely that the oxoaceto group stabilizes the active conformation of the receptor by serving as an electrophilic trap for a suitable amino acid in the side chain or that hydration of the oxoacetate should promote such stabilization.

A general trend so far is that the antagonists exhibit lower affinity (10–50 times lower) toward the AT₂ receptor compared to the agonists. Hence, the affinities are reduced when the same substituent is moved from the para-position to the meta-position. As a reference, the analogue to **86** in which the same substituent is positioned in the para-position of the phenyl ring has almost 20-fold higher AT₂ receptor affinity and presents a K_i of 3.1 nM.⁴⁰ Further optimization of the substituent in the meta-position could possibly lead to high affinity antagonists. The potential clinical significance of selective druglike AT₂ receptor antagonist still remains to be elucidated.

The SAR in the two series is not very clear. However, from series 1 it can be concluded that a nitrogen in the 3-position of the heterocycle is important for good binding, since all compounds lacking a nitrogen atom in this position (**47**–**50**) have about 10 times higher K_i, for example, **47** versus **38** and **50** versus **51**. It can also be concluded that the carbonyl group is important for good affinity when the linker between the phenyl and the imidazole is extended, since the ethylenimidazole has 5 times higher K_i compared to the corresponding carbonyl containing compound (**81** vs **73**). In the second series, with linear amides as substituents, the free rotation around the bonds between the central phenyl ring of the compounds and the nitrogen atom in the amide-based substituent makes a clear SAR hard to obtain. Depending on the properties of R₁ and R₂, the binding mode could be inverted with respect to which interaction with the AT₂ receptor that is the most favorable in total, considering both substituents. But it seems that the binding affinity outcome is a function of a combination of R₁ and R₂, since (a) the thiophene did increase the affinity when R₁ is a methyl group (**91** vs **87**), (b) extending R₁ to an ethyl group did not affect the binding affinity in the acetamide-based substituents (**93** vs **87**), and (c) the thiophene substituent did decrease the affinity when R₁ is equal to a benzyl group (**96** vs **101**) while the affinity improved 300 times when the thiophene in R₂ was kept and R₁ was exchanged from benzyl to ethyl (**101** vs **102**). It also seems like the amide in series 2 is not interchangeable with a sulfonamide in the interaction with the

AT₂ receptor, even though these two groups often are considered to be bioisosteric.

SUMMARY

In conclusion, 41 new selective and high affinity AT₂ receptor ligands have been synthesized and biologically evaluated. Five of these ligands were evaluated in a functional assay relying on neurite outgrowth. One ligand acted as an agonist and four ligands as antagonists at the AT₂ receptor. The functional response was found to be determined by the position of the substituents of the central phenyl ring, where a meta-substitution pattern could provide antagonists while the previously reported agonists have a para-substitution pattern as a characteristic feature. No antagonists were identified in the latter series.^{21,31,39–42} The antagonist **38** is considerably more effective in the assay used herein than PD 123,319 and should exhibit similar pharmacokinetic properties to **1**, thus considerably facilitating studies in more complex animal models.

We believe that these new druglike antagonists reported herein and the structurally similar agonist **1** previously reported will serve as valuable tools in the continuing assessment of the role of the AT₂ receptor in physiological systems.

EXPERIMENTAL SECTION

Chemistry. General Considerations. ¹H and ¹³C NMR spectra were recorded on a JEOL JNM-EX 270 spectrometer at 270.2 and 67.8 MHz, respectively. Chemical shifts are given as δ values (ppm) downfield from tetramethylsilane. Infrared spectra were recorded on a Perkin-Elmer model 1605 FT-IR with a compression cell and are reported as λ_{max} (cm⁻¹). For neat solids the instrument was equipped with a microfocus beam condenser with ZnSe lenses in a Diasqueeze plus diamond compressor cell (Graseby Specac Inc., Woodstock, GA, U.S.). Elemental analyses were performed by Mikro Kemi AB, Uppsala, Sweden, or Analytische Laboratorien, Lindlar, Germany. All compounds were confirmed to have >95% purity. Flash column chromatography was performed on silica gel 60 (0.04–0.063 mm, E. Merck). Thin-layer chromatography was performed on precoated silica gel F-254 plates (0.25 mm, E. Merck) and was visualized with UV light. Analytical RP-LC/MS was performed on a Gilson HPLC system with a Zorbax SB-C8, 5 μ m, 4.6 mm \times 50 mm (Agilent Technologies) column, with a Finnigan AQA quadrupole mass spectrometer at a flow rate of 1.5 mL/min (H₂O/CH₃CN/0.05% HCOOH). All the organic phases were dried over MgSO₄ unless otherwise stated. All chemicals were purchased from commercial suppliers and used directly without further purification.

3-(3-Hydroxymethylphenyl)-5-isobutylthiophene-2-(*N*-tert-butyl)sulfonamide (8**).** A mixture of *m*-bromobenzyl alcohol (1.05 g, 5.80 mmol), **7** (2.41 g, 7.56 mmol), Pd(PPh₃)₄ (270 mg, 0.234 mmol), NaOH (19.1 mL, 1.5 M aq), EtOH (5.0 mL), and toluene (30 mL) was stirred under N₂(g) at 90 °C for 4 h. After the mixture was cooled, water (10 mL) was added. The aqueous portion was extracted with ethyl acetate. The organic layer was concentrated and purified by column chromatography (EtOAc/hexane, 30:70) to give **8** as a colorless syrup (1.26 g, 3.31 mmol, 57%). ¹H NMR (CDCl₃) δ : 0.96 (d, *J* = 6.6 Hz, 6H), 0.98 (s, 9H), 1.82–2.00 (m, 1H), 2.66 (d, *J* = 7.1 Hz, 2H), 3.28 (br s, 1H), 4.67 (s, 2H), 4.81 (br s, 1H), 6.76 (s, 1H), 7.30–7.50 (m, 3H), 7.64 (s, 1H). ¹³C NMR (CDCl₃) δ : 22.1, 29.4, 30.4, 39.1, 54.4, 64.6, 127.1, 127.8, 128.5, 129.0, 134.9, 136.2, 141.2, 143.2, 148.2. IR (cm⁻¹) ν : 3498, 3286, 2958, 2870, 1465, 1313. Anal. Calcd for C₁₉H₂₇NO₃S₂: C, 59.8; H, 7.1; N, 3.7. Found: C, 60.1; H, 7.3; N, 3.9.

3-(3-Bromomethylphenyl)-5-isobutylthiophene-2-(*N*-tert-butyl)sulfonamide (9**).** A mixture of **8** (246 mg, 0.644 mmol), CBr₄ (534 mg, 1.61 mmol), and PPh₃ (422 mg, 1.61 mmol) in DMF (5.0 mL) was stirred at room temperature overnight. Then water (10 mL) was added and extracted with ethyl acetate. The organic layer was washed with water twice to remove excess DMF. Concentration and

purification by column chromatography (EtOAc/hexane, 10:90) gave **9** as a white solid (273 mg, 0.612 mmol, 95%). ¹H NMR (CDCl₃) δ : 0.97 (d, *J* = 6.3 Hz, 6H), 0.98 (s, 12H), 1.84–2.00 (m, 1H), 2.69 (d, *J* = 7.1 Hz, 2H), 4.18 (br s, 1H), 4.54 (s, 2H), 6.78 (s, 1H), 7.37–7.44 (2H, m), 7.50–7.56 (m, 1H), 7.69 (br s, 1H). ¹³C NMR (CDCl₃) δ : 22.2, 29.5, 30.5, 33.3, 39.2, 54.4, 128.6, 128.8, 128.97, 129.02, 129.7, 135.5, 136.8, 138.3, 142.1, 148.5. IR (cm⁻¹) ν : 3296, 2969, 2870, 1586, 1452, 1303. Anal. Calcd for C₁₉H₂₆BrNO₃S₂: C, 51.3; H, 5.9; N, 3.2. Found: C, 51.4; H, 6.0; N, 3.2.

General Procedure for the Synthesis of Compounds 10–13, 16, and 19. To a solution of **9** in 1,4-dioxane (2 mL), the appropriate heterocycle was added. The reaction mixture was stirred at 80 °C until the reaction was completed. The reaction mixture was concentrated under vacuum, and the crude product was purified by column chromatography to afford the products **10–13**, **16**, and **19**.

3-(3-Imidazol-1-ylmethylphenyl)-5-isobutylthiophene-2-(*N*-tert-butyl)sulfonamide (10**).** Compound **10** was synthesized from **9** (58 mg, 0.13 mmol) following the general procedure with imidazole (22 mg, 0.33 mmol) as heterocycle with a reaction time of 1 h. The crude product was purified (MeOH/CH₂Cl₂, 5:95) to afford **10** as a colorless syrup (38.4 mg, 89.0 μ mol, 68%). ¹H NMR (CDCl₃) δ : 0.85–1.05 (m, 15H), 1.80–2.00 (m, 1H), 2.66 (d, *J* = 7.1 Hz, 2H), 4.38 (s, 1H), 5.19 (s, 2H), 6.72 (s, 1H), 6.99 (s, 1H), 7.10 (s, 1H), 7.22 (app d, *J* = 7.6 Hz, 1H), 7.41 (app t, *J* = 7.6 Hz, 1H), 7.47–7.55 (m, 2H), 7.82 (s, 1H). ¹³C NMR (CDCl₃) δ : 22.1, 29.5, 30.5, 39.1, 51.0, 54.5, 119.3, 127.4, 128.4, 128.9, 128.7, 129.1, 135.6, 136.2, 136.7, 137.1, 142.3, 148.6. IR (cm⁻¹) ν : 3287, 3063, 2961, 1439, 1311. Anal. Calcd for C₂₂H₂₉N₃O₃S₂: C, 61.2; H, 6.8; N, 9.7. Found: C, 61.0; H, 6.6; N, 9.8.

General Procedure for the Synthesis of Compounds 14, 15, 17, 18, 20–23, 52. To the appropriate heterocycle dissolved in DMSO (1 mL) was added base (*t*-BuOK, KOH, or NaOH), and the mixture was stirred for 40 min at ambient temperature. This solution was added dropwise to a stirred solution of **9** in DMSO (1 mL). The reaction mixture was stirred at ambient temperature until the reaction was completed. CH₂Cl₂ (15 mL) was added, and the reaction mixture was washed with water. The organic phase was dried and concentration under vacuum, and the crude product was purified by column chromatography to afford the products **14**, **15**, **17**, **18**, **20–23**, **52**.

3-[3-(2-Bromoimidazol-1-ylmethyl)phenyl]-5-isobutylthiophene-2-(*N*-tert-butyl)sulfonamide (52**).** Compound **52** was synthesized from **9** (173.6 mg, 0.391 mmol) following the general procedure with 2-bromoimidazole (68.9 mg, 0.469 mmol) as heterocycle and NaOH (33 mg, 0.82 mmol) as base with a reaction time of 1 h. The crude product was purified (MeOH/CH₂Cl₂, 4:96) to afford **52** as a colorless syrup (197.3 mg, 0.386 mmol, 99%). ¹H NMR (CDCl₃) δ : 0.94 (s, 9H), 0.96 (d, *J* = 6.8 Hz, 6H), 1.82–2.00 (m, 1H), 2.67 (d, *J* = 7.1 Hz, 2H), 4.03 (br s, 1H), 5.14 (s, 2H), 6.73 (s, 1H), 7.05 (s, 1H), 7.08 (s, 1H), 7.22 (d, *J* = 7.6 Hz, 1H), 7.42 (app t, *J* = 7.6 Hz, 1H), 7.45–7.57 (m, 2H). ¹³C NMR (CDCl₃) δ : 22.1, 29.5, 30.5, 39.1, 51.1, 54.5, 119.6, 122.3, 127.4, 128.2, 128.7, 128.9, 129.1, 130.4, 135.7, 135.9, 136.7, 142.2, 148.6. IR (cm⁻¹) ν : 3287, 3113, 2961, 2870, 1465, 1433, 1387, 1318. Anal. Calcd for C₂₂H₂₈BrN₃O₃S₂: C, 51.8; H, 5.5; N, 8.2. Found: C, 51.7; H, 5.6; N, 8.1.

General Procedure for the Synthesis of Compounds 38, 40, 44–51. To a solution of the *tert*-butylsulfonamide (**10**, **12**, **16–23**) in CH₂Cl₂ (2 mL) was added BCl₃ (0.6 mL, 1.0 M in hexane). The reaction mixture was stirred at ambient temperature for 1 h. The reaction mixture was concentrated under vacuum. Water (5 mL) was added. The aqueous portion was extracted with EtOAc, and the combined organic phase was washed with water, brine, and water. The organic phase was dried and concentrated under vacuum. To the crude primary sulfonamides (**24**, **26**, **30–37**) were added pyrrolidienopyridine (2 equiv) and pyridine (1.5 mL), and the solution was stirred for 30 min. *n*-Butyl chloroformate (10 equiv) was added, and the mixture was stirred overnight at room temperature. Citric acid (10% aq) was added, and the reaction mixture was extracted with EtOAc and concentrated under vacuum. The crude product was purified by

column chromatography or by preparative LC–MS to obtain the products **38**, **40**, **44**–**51**.

3-[3-(Imidazol-1-ylmethylphenyl)-5-isobutylthiophene-2-(*N*-butyloxycarbonyl)sulfonamide (38**)]**. Compound **38** was synthesized from **10** (68.8 mg, 0.159 mmol) following the general procedure. The crude product was purified with column chromatography (MeOH/CH₂Cl₂, 6:94) to afford **38** (44.4 mg, 93.3 μmol, 59%). ¹H NMR (CDCl₃) δ: 0.86 (t, *J* = 7.3 Hz, 3H), 0.97 (d, *J* = 6.6 Hz, 6H), 1.18–1.34 (m, 2H), 1.44–1.58 (m, 2H), 1.84–2.00 (m, 1H), 2.67 (d, *J* = 7.1 Hz, 2H), 4.01 (t, *J* = 6.6 Hz, 2H), 4.93 (s, 2H), 6.69 (s, 1H), 6.76–7.10 (m, 3H), 7.17 (app t, *J* = 7.6 Hz, 1H), 7.32 (d, *J* = 7.6 Hz, 1H), 7.52 (s, 1H), 7.61 (br s, 1H), 12.9 (br s, 1H). ¹³C NMR (CDCl₃) δ: 13.7, 18.9, 22.2, 30.4, 30.7, 39.2, 51.1, 65.7, 119.6, 125.6, 126.5, 128.5, 128.8, 129.0, 129.3, 134.1, 134.7, 135.6, 136.2, 143.6, 149.7, 153.5. IR (cm⁻¹) ν: 3130, 3057, 2958, 1740, 1656, 1450, 1344. Anal. Calcd for C₂₃H₂₉N₃O₄S₂: C, 58.1; H, 6.2; N, 8.8. Found: C, 57.9; H, 6.1; N, 8.7.

3-[3-(2-Chloroimidazol-1-ylmethylphenyl)-5-isobutylthiophene-2-(*N*-butyloxycarbonyl)sulfonamide (63**)]**. To the solution of **52** (44 mg, 86 μmol) in TFA (3.0 mL) were added six drops of anisole. After being stirred at room temperature for 25 h, the solution was concentrated and dried under vacuum. Then pyrrolidinopyridine (25.6 mg, 0.173 mmol) and pyridine (1.5 mL) were added, and the mixture was stirred at room temperature for about 30 min. To the solution was added *n*-butyl chloroformate (118 mg, 0.864 mmol), and the mixture was stirred for 36 h at room temperature. To the reaction mixture was added EtOAc (25 mL), and the mixture was washed with citric acid (10% aq) and water, concentrated, and purified on column chromatography (MeOH/CH₂Cl₂, 5:95) to give **63** (25 mg, 49 μmol, 57%). ¹H NMR (CDCl₃) δ: 0.87 (t, *J* = 7.3 Hz, 3H), 0.99 (d, *J* = 6.6 Hz, 6H), 1.15–1.33 (m, 2H), 1.45–1.60 (m, 2H), 1.85–2.02 (m, 1H), 2.70 (d, *J* = 7.1 Hz, 2H), 4.04 (t, *J* = 6.6 Hz, 2H), 5.08 (s, 2H), 6.73 (s, 1H), 6.87 (d, *J* = 1.5 Hz, 1H), 6.90 (d, *J* = 1.5 Hz, 1H), 7.08–7.18 (m, 1H), 7.27–7.45 (m, 3H). ¹³C NMR (CDCl₃) δ: 13.6, 18.7, 22.2, 30.4, 30.5, 39.2, 49.9, 66.8, 121.2, 127.4, 128.2, 128.4, 128.9, 129.2, 131.4, 131.9, 134.9, 135.3, 145.4, 150.7, 151.5. IR (cm⁻¹) ν: 3126, 3043, 2959, 2871, 1740, 1608, 1587, 1474, 1389, 1344. Anal. Calcd for C₂₃H₂₈ClN₃O₄S₂: C, 54.2; H, 5.5; N, 8.2. Found: C, 53.9; H, 5.7; N, 8.1.

General Procedure for the Synthesis of Compounds **64**–**66**.

To a solution of 3-boromophenacyl bromide (120 mg, 0.432 mmol) in dioxane (2 mL), the appropriate heterocycle (2 equiv) was added. The reaction mixture was stirred for 1 h at 80 °C. The reaction mixture was concentrated and the crude product was purified on column chromatography to give the corresponding products **64**–**66**.

2-Benzoimidazol-1-yl-1-(3-bromophenyl)ethanone (**66**).

Compound **66** was synthesized following the general procedure with benzoimidazole (102 mg, 0.864 mmol) as heterocycle. The crude product was purified (MeOH/CH₂Cl₂, 6:94) to afford **66** (71.8 mg, 0.228 mmol, 53%). ¹H NMR (CDCl₃) δ: 5.38 (s, 2H), 7.02–7.12 (m, 1H), 7.12–7.26 (m, 2H), 7.33 (app t, *J* = 7.9 Hz, 1H), 7.60–7.86 (m, 4H), 8.02–8.12 (m, 1H). ¹³C NMR (CDCl₃) δ: 50.3, 109.2, 120.5, 122.4, 123.3, 123.4, 126.4, 130.7, 131.0, 134.0, 135.7, 137.2, 143.4, 143.6, 190.1. IR (cm⁻¹) ν: 3090, 3056, 2926, 1708, 1615, 1566, 1501, 1417, 1351. Anal. Calcd for C₁₅H₁₁BrN₂O: C, 57.2; H, 3.5; N, 8.9. Found: C, 56.9; H, 3.6; N, 8.8.

3-[3-(2-Benzoimidazol-1-ylacetyl)phenyl]-5-isobutylthiophene-2-(*N*-*tert*-butyl)sulfonamide (69**)]**. A mixture of **66** (42.7 mg, 0.136 mmol), **7** (73.5 mg, 0.230 mmol), Pd(PPh₃)₄ (9.4 mg, 8.1 μmol), Na₂CO₃ (271 μL, 0.542 mmol, 2.0 M aq), EtOH (1 mL), and toluene (7 mL) was stirred under N₂ at 80 °C for 3 h. After the mixture was cooled, water (10 mL) was added and extracted with ethyl acetate. The organic phase was dried and concentrated under vacuum and purified by column chromatography (MeOH/CH₂Cl₂, 5:95) to give **69** as a colorless syrup (62 mg, 0.122 mmol, 90%). ¹H NMR (CDCl₃) δ: 0.99 (d, *J* = 6.6 Hz, 6H), 1.08 (s, 9H), 1.86–2.02 (m, 1H), 2.71 (d, *J* = 6.9 Hz, 2H), 4.22 (br s, 1H), 5.63 (s, 2H), 6.80 (s, 1H), 7.18–7.34 (m, 3H), 7.62 (app d, *J* = 7.7 Hz, 1H), 7.76–7.90 (m, 2H), 7.97 (d, *J* = 4.3 Hz, 1H), 8.02–8.09 (m, 1H), 8.35–8.45 (m, 1H). ¹³C NMR (CDCl₃) δ: 22.1, 29.7, 30.5, 39.1, 50.4, 54.8, 109.4, 120.3, 122.3,

123.2, 127.7, 128.8, 129.1, 129.3, 134.0, 134.1, 134.4, 135.7, 137.3, 141.9, 143.1, 143.9, 149.0, 191.4. IR (cm⁻¹) ν: 3277, 3065, 2961, 2869, 1702, 1616, 1580, 1498, 1461, 1312. Anal. Calcd for C₂₇H₃₁N₃O₃S₂: C, 63.6; H, 6.1; N, 8.2. Found: C, 63.4; H, 6.1; N, 8.2.

3-[3-(2-Benzoimidazol-1-ylacetyl)phenyl]-5-isobutylthiophene-2-(*N*-*tert*-butyl)sulfonamide (75**)]**. To the solution of **69** (54.4 mg, 0.107 mmol) in TFA (3 mL) were added six drops of anisole. After being stirred at room temperature for 28 h, the solution was concentrated. To the crude product were added pyrrolidinopyridine (31.6 mg, 0.214 mmol) and pyridine (1.5 mL), and the mixture was stirred at room temperature for about 30 min. *n*-Butyl chloroformate (146 mg, 1.07 mmol) was then added to the solution and stirred at room temperature overnight. Another portion of pyrrolidinopyridine (31.6 mg, 0.214 mmol) and *n*-butyl chloroformate (146 mg, 1.07 mmol) was added and stirred for another night. To the mixture was added citric acid (10 mL 10% aq), and the mixture was extracted with ethyl acetate, concentrated, and purified by column chromatography (MeOH/CH₂Cl₂, 5:95) to give **75** (21 mg, 38 μmol, 36%). ¹H NMR (CDCl₃) δ: 0.84 (t, *J* = 7.3 Hz, 3H), 1.01 (d, *J* = 6.6 Hz, 6H), 1.14–1.34 (m, 2H), 1.42–1.60 (m, 2H), 1.86–2.02 (m, 1H), 2.72 (d, *J* = 6.9 Hz, 2H), 4.07 (t, *J* = 6.4 Hz, 2H), 6.78 (s, 1H), 7.04–7.30 (m, 3H), 7.37 (app t, *J* = 7.7 Hz, 1H), 7.45 (d, *J* = 7.7 Hz, 1H), 7.52–7.70 (m, 2H), 7.81 (s, 1H), 8.33 (s, 1H), 8.89 (br s, 1H). ¹³C NMR (CDCl₃) δ: 13.6, 18.8, 22.3, 30.5, 30.6, 39.3, 49.9, 66.1, 109.7, 119.6, 122.8, 123.7, 127.6, 128.9, 129.5, 133.4, 133.6, 133.9, 134.2, 135.3, 140.4, 143.4, 143.8, 150.7, 152.5, 190.7. IR (cm⁻¹) ν: 3061, 2959, 2871, 1739, 1702, 1604, 1580, 1499, 1462, 1343, 1289. Anal. Calcd for C₂₈H₃₁N₃O₃S₂: C, 60.7; H, 5.6; N, 7.6. Found: C, 60.5; H, 5.6; N, 7.6.

3-[3-Formyl]phenyl-5-isobutylthiophene-2-(*N*-*tert*-butyl)sulfonamide (82**)]**. A mixture of Pd(OAc)₂ (85 mg, 0.38 mmol) and PPh₃ (0.4 g, 1.5 mmol) was stirred in DME (5 mL) under N₂ (g). After being stirred for 30 min, the suspension was introduced via syringe into a nitrogen-flushed mixture of **7** (4.0 g, 13 mmol), 3-bromobenzaldehyde (2.96 mL, 25.1 mmol), and K₂CO₃ (5.21 g, 37.7 mmol) in a solvent mixture of DME, ethanol, and water (28, 8, 12 mL). After being stirred for 12 h at reflux under N₂ atmosphere, the reaction mixture was diluted with 1 M NaOH solution (50 mL) followed by ethyl acetate (150 mL). The organic layer was washed with water, and brine, dried over anhydrous MgSO₄, and concentrated in vacuo and the residue subjected to flash chromatography (20% ethyl acetate in petroleum ether) to afford **82** as a colorless solid (3.9 g, 10 mmol, 82%). ¹H NMR (CDCl₃) δ: 0.98 (d, *J* = 6.6 Hz, 6H), 1.03 (s, 9H), 1.93 (m, 1H), 2.69 (d, *J* = 6.6 Hz, 2H), 4.22 (br s, 1H), 6.79 (s, 1H), 7.61 (t, *J* = 7.9 Hz, 1H), 7.88–7.98 (m, 2H), 8.04 (t, *J* = 1.7 Hz, 1H), 10.05 (s, 1H). ¹³C NMR (CDCl₃) δ: 22.1, 29.6, 30.5, 39.1, 54.8, 128.9, 129.1, 129.4, 130.0, 135.2, 135.9, 136.3, 137.0, 141.8, 148.9, 192.0. IR (cm⁻¹) ν: 2960, 1701, 1391, 1319, 1144, 1052. Anal. Calcd for C₁₉H₂₅NO₃S₂: C, 60.1; H, 6.6; N, 3.7. Found: C, 60.4; H, 6.7; N, 3.7.

General Procedure for the Synthesis of Compounds **86**–**104**.

Step 1. To a solution of **82** (50 mg, 0.13 mmol) in MeOH (1 mL) taken in a sample vial (5 mL size), amine (1.1 equiv, 0.14 mmol) was added. After the mixture was stirred for 30 min, NaBH₄ (5 mg, 0.1 mmol) was added. The stirring continued for 30 min. The mixture was acidified with dilute HCl (5 M, 0.2 mL) and then neutralized with saturated NaHCO₃ solution (~0.5 mL) and diluted with ethyl acetate (10 mL). The contents were poured into diatomaceous earth (solid–liquid extraction cartridge) in a polypropylene column (packed for 1.5 cm, 24 mL size) and eluted with ethyl acetate (15 mL). Concentration of the filtrate under vacuum afforded the crude product.

Step 2. The preceding product was dissolved in dry CH₂Cl₂ (2 mL) in a sample vial (5 mL size). Triethylamine (36 μL, 0.26 mmol) and acid chloride (2 equiv, 0.16 mmol) were then added sequentially. The sample vial was tightly closed, and the mixture was stirred for 2 h. Water (1 mL) was added followed by ethyl acetate (5 mL), and the mixture was filtered through diatomaceous earth (packed for 1.5 cm in a column of 24 mL capacity) and eluted with CH₂Cl₂ (20 mL).

Concentration of the filtrate under vacuum afforded the crude product.

Step 3. A mixture of the above product and anisole (~2 drops) in trifluoroacetic acid (1.5 mL) in a sample vial (5 mL size) was stirred at room temperature overnight. After removal of the solvent under vacuum, the residue was dissolved in acetonitrile (2 mL) and evaporated (2×).

Step 4. To a mixture of the preceding product in dry CH₂Cl₂ (2 mL), pyrrolidinopyridine (2 mg, 0.01 mmol), triethylamine (54 μL, 0.39 mmol), and *n*-butyl chloroformate (34 μL, 0.26 mmol) were sequentially added. The solution was stirred for 2 h and concentrated under vacuum, and the crude product was purified by preparative LC–MS to afford the products **86–104**.

3-[3-(*N*-Ethoxyoxalyl,*N*-methyl)aminomethyl]phenyl-5-isobutylthiophene-2-(*N*-butyloxycarbonyl)sulfonamide (90). Compound **90** was synthesized from **82** following the general procedure with methylamine and ethyloxalyl chloride as reagents. The crude product in the final step was purified (45–75% aqueous acetonitrile) to afford **90** as a colorless oil (52 mg, 95 μmol, 73%). ¹H NMR (CDCl₃) δ: 0.87 (t, *J* = 7.3 Hz, 3H), 0.98 (dd, *J* = 2.0 Hz, *J* = 6.6 Hz, 6H), 1.18–1.41 (m, 5H), 1.53 (m, 2H), 1.94 (m, 1H), 2.70 (dd, *J* = 1.7 Hz, *J* = 6.9 Hz, 2H), 2.91 and 3.04 (s, 3H, rotation isomers), 4.05 (t, *J* = 6.6 Hz, 2H), 4.35 (dq, *J* = 2.3 Hz, *J* = 6.9 Hz, 2H), 4.49 and 4.58 (s, 2H, rotation isomers), 6.79 (m, 1H), 7.26–7.44 (m, 3H), 7.49 and 7.62 (s, 1H, rotation isomers). ¹³C NMR (CDCl₃) δ: 13.6, 13.9, 18.7, 22.2, 30.5, 32.2, 35.5, 39.3, 50.6, 53.5, 62.4, 62.7, 66.6, 66.7, 127.6, 128.2, 128.3, 128.4, 128.6, 128.7, 129.0, 129.5, 131.1, 134.6, 134.8, 135.2, 135.5, 145.3, 145.5, 150.4, 150.6, 151.5, 151.6, 161.7, 162.0, 162.5, 163.5. IR (cm⁻¹) ν: 2960, 2159, 2032, 1977, 1747, 1658, 1446, 1347, 1219, 1157. Anal. Calcd for C₂₅H₃₄N₂O₇S₂: C, 55.7; H, 6.4; N, 5.2; Found: C, 55.6; H, 6.4; N, 5.1.

3-[3-(*N*-Benzoyl,*N*-[3-picolyl]aminomethyl)phenyl-5-isobutylthiophene-2-(*N*-butyloxycarbonyl)sulfonamide (100). Compound **100** was synthesized from **82** following the general procedure with 3-picolylamine and benzoyl chloride as reagents. The crude product in the final step was purified (55–85% aqueous acetonitrile) to afford **100** as a colorless solid (52 mg, 85 μmol, 65%). Mp 73–75 °C. ¹H NMR (CDCl₃) δ: 0.89 (t, 7.3 Hz, 3H), 0.97 (d, *J* = 6.6 Hz, 6H), 1.31 (m, 2H), 1.59 (m, 2H), 1.91 (m, 1H), 2.67 (d, *J* = 6.9 Hz, 2H), 4.11 (t, *J* = 6.6 Hz, 2H), 4.74 (br m, 4H), 6.46–7.08 (br m, 4H), 7.20 (br s, 2H), 7.33–7.6 (m, 6H), 7.64–8.33 (m, 2H). ¹³C NMR (CDCl₃) δ: 13.6, 18.9, 22.2, 30.5, 30.6, 39.2, 47.9, 50.2, 52.3, 54.5, 66.0, 123.6, 126.8, 127.8, 128.7, 129.5, 129.8, 132.2, 132.7, 134.8, 135.6, 136.1, 137.1, 137.9, 145.0, 146.4, 147.2, 149.4, 150.5, 151.7, 172.5. IR (cm⁻¹) ν: 2960, 1740, 1635, 1412, 1345, 1157, 733. Anal. Calcd for C₃₃H₃₇N₃O₅S₂·H₂O: C, 62.1; H, 6.2; N, 6.6; Found: C, 62.0; H, 6.0; N, 6.2.

Rat Liver Membrane AT₁ Receptor-Binding Assay. Rat liver membranes were prepared according to the method of Dudley et al.⁴⁶ Binding of [¹²⁵I]Ang II to membranes was conducted in a final volume of 0.5 mL containing 50 mM Tris-HCl (pH 7.4), 100 mM NaCl, 10 mM MgCl₂, 1 mM EDTA, 0.025% bacitracin, 0.2% BSA (bovine serum albumin), liver homogenate corresponding to 5 mg of the original tissue weight, [¹²⁵I]Ang II (80000–85000 cpm, 0.03 nM), and variable concentrations of test substance. Samples were incubated at 25 °C for 2 h, and binding was terminated by filtration through Whatman GF/B glass-fiber filter sheets, which had been presoaked overnight with 0.3% polyethylamine, using a Brandel cell harvester. The filters were washed with 3 × 3 mL of Tris-HCl (pH 7.4) and transferred into tubes. The radioactivity was measured in a μ-counter. The characteristics of the Ang II binding AT₁ receptor was determined by using six different concentrations (0.03–5 nmol/L) of the labeled [¹²⁵I]Ang II. Nonspecific binding was determined in the presence of 1 μM Ang II. The specific binding was determined by subtracting the nonspecific binding from the total bound [¹²⁵I]Ang II. The apparent dissociation constant *K_d* values were calculated from IC₅₀ values using the Cheng–Prusoff equation (*K_d* = 1.7 ± 0.1 nM, [L] = 0.057 nM). The binding data were best fitted with a one-site fit. All determinations were performed in triplicate.

Porcine (Pig) Myometrial Membrane AT₂ Receptor-Binding Assay. Myometrial membranes were prepared from porcine uteri according to the method by Nielsen et al.⁴⁷ A presumable interference by binding to AT₁ receptors was blocked by addition of 1 μM losartan. Binding of [¹²⁵I]Ang II to membranes was conducted in a final volume of 0.5 mL containing 50 mM Tris-HCl (pH 7.4), 100 mM NaCl, 10 mM MgCl₂, 1 mM EDTA, 0.025% bacitracin, 0.2% BSA, homogenate corresponding to 10 mg of the original tissue weight, [¹²⁵I]Ang II (80000–85000 cpm, 0.03 nM), and variable concentrations of test substance. Samples were incubated at 25 °C for 1.5 h, and binding was terminated by filtration through Whatman GF/B glass-fiber filter sheets, which had been presoaked overnight with 0.3% polyethylamine, using a Brandel cell harvester. The filters were washed with 3 × 3 mL of Tris-HCl (pH 7.4) and transferred into tubes. The radioactivity was measured in a μ-counter. The characteristics of the Ang II binding AT₂ receptor was determined by using six different concentrations (0.03–5 nmol/L) of the labeled [¹²⁵I]Ang II. Nonspecific binding was determined in the presence of 1 μM Ang II. The specific binding was determined by subtracting the nonspecific binding from the total bound [¹²⁵I]Ang II. The apparent dissociation constant *K_d* values were calculated from IC₅₀ values using the Cheng–Prusoff equation (*K_d* = 0.73 ± 0.06 nM, [L] = 0.057 nM). The binding data were best fitted with a one-site fit. All determinations were performed in triplicate.

In Vitro Morphological Effects. General. The chemicals used in the present study were obtained from the following sources: Dulbecco's modified Eagle's medium (DMEM), heat-inactivated fetal bovine serum (FBS), HAT supplement (hypoxanthine, aminopterin, thymidine), gentamycin from Gibco BRL (Burlington, Ontario, Canada), and [Val⁵]angiotensin II from Bachem (Marina Delphen, CA, U.S.). PD 123,319 was obtained from RBI (Natick, MA, U.S.). All other chemicals were of grade A purity.

Cell Culture. To study the in vitro morphological effects, NG108-15 cells (initially provided by Drs. M. Emerit and M. Hamon; INSERM, U. 238, Paris, France) were used as well as transfected NG108-15/pcDNA3 cells. The transfected cell line has previously been shown to have the same behavior as the native cell line.²⁸ Both cell lines were cultured (NG108-15 passage 18–28, NG108-15/pcDNA3 passage 12–18) in Dulbecco's modified Eagle's medium (DMEM, Gibco BRL, Burlington, Ontario, Canada) with 10% fetal bovine serum (FBS, Gibco), HAT supplement (hypoxanthine, aminopterin, thymidine from Gibco), and 50 mg/L gentamycin (Gibco) at 37 °C in 75 cm² Nunclon Δ flasks in a humidified atmosphere of 93% air and 7% CO₂, as previously described.^{28,48} The transfected cell line was kept stable by addition of Geneticin (G-418, 200 μg/mL) to the medium.²⁸ Subcultures were performed at subconfluency. Under these conditions, cells express only the AT₂ receptor subtype.^{28,48} Cells were stimulated during 3 days, once a day (first stimulation 24 h after plating). Cells were cultured for 3 subsequent days under these conditions. For all experiments, cells were plated at the same initial density of 3.6 × 10⁴ cells/35 mm Petri dish. To determine a good test concentration, compounds **38**, **63**, **75**, **90**, and **100** were tested at various concentrations ranging from 1 pM to 1 μM. For all the compounds it was only at the highest concentration that the tendency of cell death was observed. Cells were treated without (control cells) or with [Val⁵]angiotensin II from Bachem (Marina Delphen, CA, U.S.) (100 nM) or **38** (10 nM), **63** (10 nM), **75** (10 nM), **90** (1 nM), and **100** (10 nM) in the absence or in the presence of PD 123,319 (RBI Natick, MA, U.S.) (10 μM), an AT₂ receptor antagonist introduced daily 30 min prior to Ang II, **38**, **63**, **75**, **90**, or **100**. During the 3 days of treatment the transfected cell line was cultured without Geneticin.

Determination of Cells with Neurites. Cells were examined under a phase contrast microscope, and micrographs were taken after 3 days under the various experimental conditions. Cells with at least one neurite longer than a cell body were counted as positive for neurite outgrowth. The number of cells with neurites represents the percentage of the total amount of cells in the micrographs. At least three different experiments were conducted for each condition, each in duplicate. At least five images were taken per Petri dish; hence, a total of 250–400 cells from each of the duplicate dishes were examined.

The data are represented as the mean \pm SEM of the average number of cells on a micrograph.

Data Analysis. The data are presented as the mean \pm SEM of the average number of cells on a micrograph. Statistical analyses of the data were performed using the two-way ANOVA test. Homogeneity of variance was assessed by Bartlett's test, and *p* values were obtained from Dunnett's tables.

■ ASSOCIATED CONTENT

● Supporting Information

Synthesis procedures and characterization of all compounds and procedures for the biological evaluations. This material is available free of charge via the Internet at <http://pubs.acs.org>.

■ AUTHOR INFORMATION

Corresponding Author

*For N.G.-P.: phone, +1-819-5645243; e-mail, nicole.gallopayet@usherbrooke.ca. For A.H.: phone, +46-18-4714284; e-mail, anders.hallberg@orgfarm.uu.se. For M.A.: phone, +46-18-4714124; e-mail, mathias.alterman@orgfarm.uu.se.

Notes

The authors declare no competing financial interest.

■ ACKNOWLEDGMENTS

We gratefully acknowledge support from the Swedish Research Council (VR), the Swedish Foundation for Strategic Research (SSF), Knut and Alice Wallenberg Foundation, and the Canada Research Chairs Program. N.G.-P. is a recipient of a Canada Research Chair in Endocrinology of the Adrenal Gland. N.G.-P. is member of the FRSQ-funded Centre de Recherche Clinique Étienne-le Bel. We thank Lucie Chouinard and the other members of the laboratory for their technical assistance with cell cultures.

■ REFERENCES

- (1) de Gasparo, M.; Catt, K. J.; Inagami, T.; Wright, J. W.; Unger, T. International Union of Pharmacology. XXIII. The Angiotensin II Receptors. *Pharmacol. Rev.* **2000**, *52*, 415–472.
- (2) Porrello, E. R.; Delbridge, L. M. D.; Thomas, W. G. The Angiotensin II Type 2 (AT₂) Receptor: An Enigmatic Seven Transmembrane Receptor. *Front. Biosci.* **2009**, *14*, 958–972.
- (3) Steckelings, U. M.; Kaschina, E.; Unger, T. The AT₂ Receptor—A Matter of Love and Hate. *Peptides* **2005**, *26*, 1401–1409.
- (4) Grady, E. F.; Sechi, L. A.; Griffin, C. A.; Schambelan, M.; Kalinyak, J. E. Expression of AT₂ Receptors in the Developing Rat Fetus. *J. Clin. Invest.* **1991**, *88*, 921–933.
- (5) Bastien, N. R.; Ciuffo, G. M.; Saavedra, J. M.; Lambert, C. Angiotensin II Receptor Expression in the Conduction System and Arterial Duct of Neonatal and Adult Rat Hearts. *Regul. Pept.* **1996**, *63*, 9–16.
- (6) Okumura, M.; Iwai, M.; Ide, A.; Mogi, M.; Ito, M.; Horiuchi, M. Sex Differences in Vascular Injury and the Vasoprotective Effect of Valsartan Are Related to Differential AT₂ Receptor Expression. *Hypertension* **2005**, *46*, 577–583.
- (7) Steckelings, U. M.; Henz, B. M.; Wiehstutz, S.; Unger, T.; Artuc, M. Differential Expression of Angiotensin Receptors in Human Cutaneous Wound Healing. *Br. J. Dermatol.* **2005**, *153*, 887–893.
- (8) Gallinat, S.; Yu, M.; Dorst, A.; Unger, T.; Herdegen, T. Sciatic Nerve Transection Evokes Lasting Up-Regulation of Angiotensin AT₂ and AT₁ Receptor mRNA in Adult Rat Dorsal Root Ganglia and Sciatic Nerves. *Mol. Brain Res.* **1998**, *57*, 111–122.
- (9) Vázquez, E.; Coronel, I.; Bautista, R.; Romo, E.; Villalón, C. M.; Avila-Casado, C. M.; Soto, V.; Escalante, B. Angiotensin II-Dependent Induction of AT₂ Receptor Expression after Renal Ablation. *Am. J. Physiol.: Renal Physiol.* **2005**, *288*, F207–F213.

(10) Nio, Y.; Matsubara, H.; Murasawa, S.; Kanasaki, M.; Inada, M. Regulation of Gene Transcription of Angiotensin II Receptor Subtypes in Myocardial Infarction. *J. Clin. Invest.* **1995**, *95*, 46–54.

(11) Li, J.; Culman, J.; Hortnagl, H.; Zhao, Y.; Gerova, N.; Timm, M.; Blume, A.; Zimmermann, M.; Seidel, K.; Dirnagl, U.; Unger, T. Angiotensin AT₂ Receptor Protects against Cerebral Ischemia-Induced Neuronal Injury. *FASEB J.* **2005**, *19*, 617–619.

(12) Oishi, Y.; Ozono, R.; Yano, Y.; Teranishi, Y.; Akishita, M.; Horiuchi, M.; Oshima, T.; Kambe, M. Cardioprotective Role of AT₂ Receptor in Postinfarction Left Ventricular Remodeling. *Hypertension* **2003**, *41*, 814–818.

(13) McCarthy, C. A.; Vinh, A.; Callaway, J. K.; Widdop, R. E. Angiotensin AT₂ Receptor Stimulation Causes Neuroprotection in a Conscious Rat Model of Stroke. *Stroke* **2009**, *40*, 1482–1489.

(14) Reinecke, K.; Lucius, R.; Reinecke, A.; Rickert, U.; Herdegen, T.; Unger, T. Angiotensin II Accelerates Functional Recovery in the Rat Sciatic Nerve in Vivo: Role of the AT₂ Receptor and the Transcription Factor NF- κ B. *FASEB J.* **2003**, *17*, 2094–2096.

(15) Rompe, F.; Artuc, M.; Hallberg, A.; Alterman, M.; Stroder, K.; Thone-Reinecke, C.; Reichenbach, A.; Schacherl, J.; Dahlof, B.; Bader, M.; Alenina, N.; Schwaninger, M.; Zuberbier, T.; Funke-Kaiser, H.; Schmidt, C.; Schunck, W. H.; Unger, T.; Steckelings, U. M. Direct Angiotensin II Type 2 Receptor Stimulation Acts Anti-Inflammatory through Epoxyeicosatrienoic Acid and Inhibition of Nuclear Factor κ B. *Hypertension* **2010**, *55*, 924–931.

(16) Johansson, B.; Holm, M.; Ewert, S.; Casselbrant, A.; Pettersson, A.; Fändriks, L. Type 2 Receptor-Mediated Duodenal Mucosal Alkaline Secretion in the Rat. *Am. J. Physiol.* **2001**, *280*, G1254–G1260.

(17) Gendron, L.; Payet, M.; Gallo-Payet, N. The AT₂ Receptor of Angiotensin II and Neuronal Differentiation: From Observations to Mechanisms. *J. Mol. Endocrinol.* **2003**, *31*, 359–372.

(18) Carey, R. M.; Padia, S. H. Angiotensin AT₂ Receptors: Control of Renal Sodium Excretion and Blood Pressure. *Trends Endocrinol. Metab.* **2008**, *19*, 84–87.

(19) Siragy, H. M. The Potential Role of the Angiotensin Subtype 2 Receptor in Cardiovascular Protection. *Curr. Hypertens. Rep.* **2009**, *11*, 260–262.

(20) Lemarie, C. A.; Schiffrin, E. L. The Angiotensin II Type 2 Receptor in Cardiovascular Disease. *J. Renin–Angiotensin–Aldosterone Syst.* **2010**, *11*, 19–31.

(21) Wan, Y.; Wallinder, C.; Plouffe, B.; Beaudry, H.; Mahalingam, A. K.; Wu, X.; Johansson, B.; Holm, M.; Botros, M.; Karlen, A.; Pettersson, A.; Nyberg, F.; Faendriks, L.; Gallo-Payet, N.; Hallberg, A.; Alterman, M. Design, Synthesis, and Biological Evaluation of the First Selective Nonpeptide AT₂ Receptor Agonist. *J. Med. Chem.* **2004**, *47*, 5995–6008.

(22) Kaschina, E.; Grzesiak, A.; Li, J.; Foryst-Ludwig, A.; Timm, M.; Rompe, F.; Sommerfeld, M.; Kemnitz, U. R.; Curato, C.; Namsolleck, P.; Tschöpe, C.; Hallberg, A.; Alterman, M.; Hucko, T.; Paetsch, I.; Dietrich, T.; Schnackenburg, B.; Graf, K.; Dahlof, B.; Kintscher, U.; Unger, T.; Steckelings, U. M. Angiotensin II Type 2 Receptor Stimulation: A Novel Option of Therapeutic Interference with the Renin–Angiotensin System in Myocardial Infarction? *Circulation* **2008**, *118*, 2523–2532.

(23) Steckelings, U. M.; Larhed, M.; Hallberg, A.; Widdop, R. E.; Jones, E. S.; Wallinder, C.; Namsolleck, P.; Dahlof, B.; Unger, T. Non-Peptide AT₂-Receptor Agonists. *Curr. Opin. Pharmacol.* **2010**, *11*, 187–192.

(24) Tamargo, J.; López-Sendón, J. Novel Therapeutic Targets for the Treatment of Heart Failure. *Nat. Rev. Drug Discovery* **2011**, *10*, 536–555.

(25) Steckelings, U. M.; Widdop, R. E.; Paulis, L.; Unger, T. The Angiotensin AT₂ Receptor in Left Ventricular Hypertrophy. *J. Hypertens.* **2010**, *28* (Suppl. 1), S50–S55.

(26) Unger, T.; Dahlof, B. Compound 21, the First Orally Active, Selective Agonist of the Angiotensin II Type 2 (AT₂) Receptor: Implications for AT₂ Receptor Research and Therapeutic Potential. *J. Renin–Angiotensin–Aldosterone Syst.* **2010**, *11*, 75–77.

- (27) Brechler, V.; Jones, P. W.; Levens, N. R.; de Gasparo, M.; Bottari, S. P. Agonistic and Antagonistic Properties of Angiotensin Analogs at the AT₂ Receptor in PC12W Cells. *Regul. Pept.* **1993**, *44*, 207–213.
- (28) Buisson, B.; Bottari, S. P.; de Gasparo, M.; Gallo-Payet, N.; Payet, M. D. The Angiotensin AT₂ Receptor Modulates T-Type Calcium Current in Non-Differentiated NG108-15 Cells. *FEBS Lett.* **1992**, *309*, 161–164.
- (29) Perlman, S.; Schambye, H. T.; Rivero, R. A.; Greenlee, W. J.; Hjorth, S. A.; Schwartz, T. W. Non-Peptide Angiotensin Agonist. Functional and Molecular Interaction with the AT₁ Receptor. *J. Biol. Chem.* **1995**, *270*, 1493–1496.
- (30) Kivlighn, S. D.; Huckle, W. R.; Zingaro, G. J.; Rivero, R. A.; Lotti, V. J.; Chang, R. S. L.; Schorn, T. W.; Kevin, N.; Johnson, R. G. Jr. Discovery of L-162,313: A Nonpeptide That Mimics the Biological Actions of Angiotensin II. *Am. J. Physiol.* **1995**, *268*, R820–R823.
- (31) Wan, Y.; Wallinder, C.; Johansson, B.; Holm, M.; Mahalingam, A. K.; Wu, X.; Botros, M.; Karlen, A.; Pettersson, A.; Nyberg, F.; Faendriks, L.; Hallberg, A.; Alterman, M. First Reported Nonpeptide AT₁ Receptor Agonist (L-162,313) Acts as an AT₂ Receptor Agonist in Vivo. *J. Med. Chem.* **2004**, *47*, 1536–1546.
- (32) Perlman, S.; Costa-Neto, C. M.; Miyakawa, A. A.; Schambye, H. T.; Hjort, S. A.; Paiva, A. C. M.; Rivero, R. A.; Greenlee, W. J.; Schwartz, T. W. Dual Agonistic and Antagonistic Property of Nonpeptide Angiotensin AT₁ Ligands: Susceptibility to Receptor Mutations. *Mol. Pharmacol.* **1997**, *51*, 301–311.
- (33) Rosenström, U.; Sköld, C.; Lindeberg, G.; Botros, M.; Nyberg, F.; Karlén, A.; Hallberg, A. A Selective AT₂ Receptor Ligand with a γ -Turn-like Mimetic Replacing the Amino Acid Residues 4–5 of Angiotensin II. *J. Med. Chem.* **2004**, *47*, 859–70.
- (34) Rosenström, U.; Sköld, C.; Plouffe, B.; Lindeberg, G.; Botros, M.; Nyberg, F.; Wolf, G.; Karlén, A.; Gallo-Payet, N.; Hallberg, A. New Selective AT₂ Receptor Ligands Encompassing a γ -Turn Mimetic Replacing the Amino Acid Residues 4–5 of Angiotensin II Act as Agonists. *J. Med. Chem.* **2005**, *48*, 4009–4024.
- (35) Georgsson, J.; Sköld, C.; Plouffe, B.; Lindeberg, G.; Botros, M.; Larhed, M.; Nyberg, F.; Gallo-Payet, N.; Gogoll, A.; Karlen, A.; Hallberg, A. Angiotensin II Pseudopeptides Containing 1,3,5-Trisubstituted Benzene Scaffolds with High AT₂ Receptor Affinity. *J. Med. Chem.* **2005**, *48*, 6620–6631.
- (36) Rosenström, U.; Sköld, C.; Lindeberg, G.; Botros, M.; Nyberg, F.; Karlén, A.; Hallberg, A. Design, Synthesis, and Incorporation of a β -Turn Mimetic in Angiotensin II Forming Novel Pseudopeptides with Affinity for AT₁ and AT₂ Receptors. *J. Med. Chem.* **2006**, *49*, 6133–6137.
- (37) Georgsson, J.; Rosenström, U.; Wallinder, C.; Beaudry, H.; Plouffe, B.; Lindeberg, G.; Botros, M.; Nyberg, F.; Karlen, A.; Gallo-Payet, N.; Hallberg, A. Short Pseudopeptides Containing Turn Scaffolds with High AT₂ Receptor Affinity. *Bioorg. Med. Chem.* **2006**, *14*, 5963–5972.
- (38) Georgsson, J.; Sköld, C.; Botros, M.; Lindeberg, G.; Nyberg, F.; Karlen, A.; Hallberg, A.; Larhed, M. Synthesis of a New Class of Druglike Angiotensin II C-Terminal Mimics with Affinity for the AT₂ Receptor. *J. Med. Chem.* **2007**, *50*, 1711–1715.
- (39) Wu, X.; Wan, Y.; Mahalingam, A. K.; Murugaiah, A. M. S.; Plouffe, B.; Botros, M.; Karlén, A.; Hallberg, M.; Gallo-Payet, N.; Alterman, M. Selective Angiotensin II AT₂ Receptor Agonists: Arylbenzimidazole Structure–Activity Relationships. *J. Med. Chem.* **2006**, *49*, 7160–7168.
- (40) Murugaiah, A. M. S.; Wallinder, C.; Mahalingam, A. K.; Wu, X.; Wan, Y.; Plouffe, B.; Botros, M.; Karlén, A.; Hallberg, M.; Gallo-Payet, N.; Alterman, M. Selective Angiotensin II AT₂ Receptor Agonists Devoid of the Imidazole Ring System. *Bioorg. Med. Chem.* **2007**, *15*, 7166–7183.
- (41) Wallinder, C.; Botros, M.; Rosenström, U.; Guimond, M.-O.; Beaudry, H.; Nyberg, F.; Gallo-Payet, N.; Hallberg, A.; Alterman, M. Selective Angiotensin II AT₂ Receptor Agonists: Benzamide Structure–Activity Relationships. *Bioorg. Med. Chem.* **2008**, *16*, 6841–6849.
- (42) Mahalingam, A. K.; Wan, Y.; Murugaiah, A. M. S.; Wallinder, C.; Wu, X.; Plouffe, B.; Botros, M.; Nyberg, F.; Hallberg, A.; Gallo-Payet, N.; Alterman, M. Selective Angiotensin II AT₂ Receptor Agonists with Reduced CYP 450 Inhibition. *Bioorg. Med. Chem.* **2010**, *18*, 4570–4590.
- (43) Blankley, C. J.; Hodges, J. C.; Klutchko, S. R.; Himmelsbach, R. J.; Chucholowski, A.; Connolly, C. J.; Neergaard, S. J.; Van Nieuwenhze, M. S.; Sebastian, A.; Quin, J. III; Essenburg, A. D.; Cohen, D. M. Synthesis and Structure-Activity Relationships of a Novel Series of Non-Peptide Angiotensin II Receptor Binding Inhibitors Specific for the AT₂ Subtype. *J. Med. Chem.* **1991**, *34*, 3248–3260.
- (44) Kevin, N. J.; Rivero, R. A.; Greenlee, W. J.; Chang, R. S. L.; Chen, T. B. Substituted Phenylthiophene Benzoylsulfonamides with Potent Binding Affinity to Angiotensin II AT₁ and AT₂ Receptors. *Bioorg. Med. Chem. Lett.* **1994**, *4*, 189–194.
- (45) Wan, Y.; Wu, X.; Mahalingam, A. K.; Alterman, M. Boron Trichloride as an Efficient and Selective Agent for Deprotection of *tert*-Butyl Aryl Sulfonamides. *Tetrahedron Lett.* **2003**, *44*, 4523–4525.
- (46) Dudley, D. T.; Panek, R. L.; Major, T. C.; Lu, G. H.; Bruns, R. F.; Klinkefus, B. A.; Hodges, J. C.; Weishaar, R. E. Subclasses of Angiotensin II Binding Sites and Their Functional Significance. *Mol. Pharmacol.* **1990**, *38*, 370–377.
- (47) Nielsen, A. H.; Schauser, K.; Winther, H.; Dantzer, V.; Poulsen, K. Angiotensin II Receptors and Renin in the Porcine Uterus: Myometrial AT₂ and Endometrial AT₁ Receptors Are Down-Regulated during Gestation. *Clin. Exp. Pharmacol. Physiol.* **1997**, *24*, 309–314.
- (48) Laflamme, L.; de Gasparo, M.; Gallo, J. M.; Payet, M. D.; Gallo-Payet, N. Angiotensin II Induction of Neurite Outgrowth by AT₂ Receptors in NG108-15 Cells. Effect Counteracted by the AT₁ Receptors. *J. Biol. Chem.* **1996**, *271*, 22729–22735.
- (49) Gendron, L.; Oligny, J. F.; Payet, M. D.; Gallo-Payet, N. Cyclic AMP-Independent Involvement of Rap1/B-Raf in the Angiotensin II AT₂ Receptor Signaling Pathway in NG108-15 Cells. *J. Biol. Chem.* **2003**, *278*, 3606–3614.
- (50) Gendron, L.; Laflamme, L.; Rivard, N.; Asselin, C.; Payet, M. D.; Gallo-Payet, N. Signals from the AT₂ (Angiotensin Type 2) Receptor of Angiotensin II Inhibit p21ras and Activate MAPK (Mitogen-Activated Protein Kinase) To Induce Morphological Neuronal Differentiation in NG108-15 Cells. *Mol. Endocrinol.* **1999**, *13*, 1615–1626.
- (51) Gendron, L.; Cote, F.; Payet, M. D.; Gallo-Payet, N. Nitric Oxide and Cyclic GMP are Involved in Angiotensin II AT₂ Receptor Effects on Neurite Outgrowth in NG108-15 Cells. *Neuroendocrinology* **2002**, *75*, 70–81.
- (52) Semple, G.; Fioravanti, B.; Pereira, G.; Calderon, I.; Uy, J.; Choi, K.; Xiong, Y.; Ren, A.; Morgan, M.; Dave, V.; Thomsen, W.; Unett, D. J.; Xing, C.; Bossie, S.; Carroll, C.; Chu, Z.-L.; Grottick, A. J.; Hauser, E. K.; Leonard, J.; Jones, R. M. Discovery of the First Potent and Orally Efficacious Agonist of the Orphan G-Protein Coupled Receptor 119. *J. Med. Chem.* **2008**, *51*, 5172–5175.
- (53) Sugg, E. Nonpeptide Agonists for Peptide Receptors: Lessons from Ligands. *Annu. Rep. Med. Chem.* **1997**, *32*, 277–283.
- (54) Levitzki, A.; Gazit, A. Tyrosine Kinase Inhibition: An Approach to Drug Development. *Science* **1995**, *267*, 1782–1788.
- (55) Plouffe, B.; Guimond, M.-O.; Beaudry, H.; Gallo-Payet, N. Role of Tyrosine Kinase Receptors in Angiotensin II AT₂ Receptor Signaling: Involvement in Neurite Outgrowth and in p42/p44mapk Activation in NG108-15 Cells. *Endocrinology* **2006**, *147*, 4646–4654.
- (56) The agonist M024 is also known as compound 21 (C21).